Genetic and physiological characterization of gramillin sensitivity in barley

Siddharthan Lakshmanan

Thesis submitted to the University of Ottawa
in partial fulfillment of the requirements for the
Master of Science in Biology

Department of Biology
Faculty of Science
University of Ottawa

Abstract

Microbes produce ionophores, metabolites which facilitate ion transport across membranes, to disrupt host membranes and cellular function. Plant hosts can perceive ionophore-based disruption, and some genotypes have developed ionophore insensitivity. The basis of ionophore insensitivity is unclear but could involve avoidance of membrane interaction with the ionophore, ionophore degradation or membrane recovery. Here, we describe the insensitivity of the Lowe barley against the gramillin ionophore, a virulence factor produced by *Fusarium graminearum* that induces host stress responses which then promote fungal secondary metabolite gene expression during infection. During barley leaf infection, higher *F. graminearum* trichothecene and culmorin biosynthetic gene expression was observed in gramillin-sensitive barley compared to Lowe. Lowe degrades gramillin to a similar extent as gramillin-sensitive genotypes and can induce callose production and transcriptional reprogramming in response to gramillin. However, gramillin-induced stress responses are smaller in Lowe compared to gramillin-sensitive barley genotypes. At 4 hours after gramillin treatment, only 1,175 genes are differentially expressed in Lowe compared to 3,885 in gramillin-sensitive Leo barley. Gramillin-induced callose production and defense gene induction are smaller in Lowe compared to sensitive genotypes. Inducible stress responses were not required for gramillin insensitivity in Lowe. Together, this indicates that gramillin can disrupt membranes in Lowe to induce stress responses and that Lowe insensitivity is unlikely due to complete avoidance or gramillin degradation. Instead, the toxicity of gramillin is attenuated in Lowe which aligns with lower induction of *F. graminearum* secondary metabolite biosynthetic genes during infection.

Résumé

Les microbes produisent des ionophores, des métabolites qui facilitent le transport d'ions à travers les membranes, afin de perturber les membranes de l'hôte et le fonctionnement cellulaire. Les plantes hôtes sont capables de percevoir ces perturbations induites par les ionophores, et certains génotypes ont développé une insensibilité aux ionophores. Le mécanisme à l'origine de cette insensibilité aux ionophores n'est pas clairement établi, mais pourrait impliquer la prévention de l'interaction entre la membrane et l'ionophore, la dégradation de l'ionophore ou la régénération de la membrane. Nous décrivons ici l'insensibilité de l'orge Lowe à l'ionophore gramilline, un facteur de virulence produit par Fusarium graminearum qui induit des réponses de stress chez l'hôte, lesquelles favorisent ensuite l'expression des gènes codant pour les métabolites secondaires fongiques au cours de l'infection. Au cours de l'infection des feuilles d'orge, une expression génique plus élevée des gènes impliqués dans la biosynthèse des trichothécènes et de la culmorine de F. graminearum a été observée chez l'orge sensible à la gramilline par rapport à la variété Lowe. La variété Lowe dégrade la gramilline dans une mesure similaire à celle des génotypes sensibles à la gramilline et peut induire la production de callose ainsi qu'une reprogrammation transcriptionnelle en réponse à la gramilline. Cependant, les réponses de stress induites par la gramilline sont moins marquées chez la variété Lowe que chez les génotypes d'orge sensibles à la gramilline. Quatre heures après le traitement à la gramilline, seuls 1,175 gènes présentent une expression différentielle chez la variété Lowe, contre 3,885 chez l'orge Leo sensible à la gramilline. La production de callose et l'induction des gènes de défense induites par la gramilline sont moins marquées chez la variété Lowe que

chez les génotypes sensibles. Les réponses au stress inductibles n'étaient pas nécessaires à l'insensibilité de Lowe à la gramilline. Dans l'ensemble, cela indique que la gramilline peut perturber les membranes chez Lowe afin d'induire des réponses au stress et qu'il est peu probable que l'insensibilité de Lowe soit due à une évitement complet ou à la dégradation de la gramilline. Au contraire, la toxicité de la gramilline est atténuée chez Lowe, ce qui concorde avec une induction plus faible des gènes de biosynthèse des métabolites secondaires de F. graminearum au cours de l'infection.

Acknowledgements

I would like to begin by thanking my supervisor, Dr. Elizabeth Brauer, for her guidance, mentorship and support throughout this project and beyond. I am also grateful to my committee members, Dr. David Overy and Dr. Jean-Sébastien Parent for their time and valuable discussions.

This project would not have been possible without the support of my colleagues at Agriculture and Agri-Food Canada. To Whynn Bosnich, I will always be grateful for your thoughtfulness and technical expertise throughout my project. To Marielle Zouein and Emily Marion, thank you for your friendship, many conversations and moral support. I am grateful to Nathan Liang for his assistance with the transcriptomic analysis. I thank Dr. Indira Thapa and the Blackwell Lab for mass-spec analysis of gramillin and my leaf extract samples. I also thank Dr. Thomas Witte, Amanda Sproule and the Overy Lab for their support with the metabolomic analysis, and Dr. Jason McAlister of the Geddes-McAlister laboratory at the University of Guelph for conducting the proteomic analysis. I am grateful to Martin Charette for training me in the KASP assay and to Miriko Tobori and the greenhouse staff at the Ottawa Research and Development Centre for their help in caring for my plants and collecting seed. Finally, I am deeply grateful for the support system around me: my source of inspiration and strength my mother – Dr. Parimala Doss, my sister Shubangi, my girlfriend Andrea and all my friends from Toronto to New Delhi. Thank you for your encouragement, curiosity and support throughout my academic journey. I could not have done this without you!

Table of Contents

List of Tables

List of Figures

List of Abbreviations

ABC ..... ATP-binding cassette

ATP..... Adenosine triphosphate

BGC ..... Biosynthetic gene cluster

BIK1 .....Botrytis-induced kinase 1

cDNA ..... Complementary deoxyribonucleic acid

CDPK ..... Calcium dependent protein kinase

Clm ..... Culmorin

CLP ..... Cyclic lipopeptide ionophore

DAMP ..... Damage-associated molecular pattern

DEG .....Differentially expressed gene

DNA .....Deoxyribonucleic acid

Dpi .....Days post-inoculation

DPI ..... Diphenyleneiodonium

DON .....Deoxynivalenol

ELO..... Elongation of very-long-chain fatty acids

FHB .....Fusarium Head Blight

GAPDH .....Glyceraldehyde-3-phosphate dehydrogenase

gDNA .....Genomic deoxyribonucleic acid

GO .....Gene ontology

HPLC ..... High-performance liquid chromatography

IC .....Infection cushion

ISR.....Induced systematic resistance

ILK1 .....Integrin-like kinase 1

LPS.....Lipopolysaccharide

KASP ..... Kompetitive Allele-Specific PCR

MAMP .....Microbe-associated molecular pattern

MAPK .....Mitogen-activated protein kinase

NADPH .....Nicotinamide adenine dinucleotide phosphate

NRPS .....Non-ribosomal peptide synthase

PAMP .....Pathogen associated molecular pattern

PRR.....Pattern-recognition receptor

PTI .....Pattern-triggered immunity

qPCR .....Quantitative polymerase chain reaction

QTL ..... Quantitative trait locus

RBOHD .....Respiratory burst oxidase homolog D

RLCK .....Receptor-like cytoplasmic kinase

RNA-seq .....Ribonucleic acid sequencing

ROS .....Reactive oxygen species

SHAM ..... Salicylhydroxamic acid

SNP .....Single nucleotide polymorphism

TC .....Transformation control

TRI .....Trichothecene

1. Introduction

1.1 Fusarium Head Blight: Origin and impact

Fusarium Head Blight (FHB) is a devastating fungal disease that poses a significant threat to the sustainable production of important cereal crops such as maize, wheat and barley (McMullen et al., 2012). Historically, the first known occurrence of FHB was reported in 1884 in England, followed by America, Europe, Australia, and South Africa establishing this as a global problem (Alisaac & Mahlein, 2023; Buttar et al., 2024). In Canada, FHB was first detected in 1919 while the first major outbreak was reported in the early 1980s (Zhu et al., 2019). This disease has since gone on to cost the Canadian grains industry between $50 and $300 million annually (SaskBarley, 2023). The economic impact of FHB is primarily a result of severe grain downgrading, as it promotes premature bleaching of spikelets, shriveled kernels and accumulation of mycotoxins, particularly deoxynivalenol (DON), that render crops unsuitable for consumption or industrial use (Canadian Grain Commission, 2019; Moonjely et al., 2023). Despite decades of research and global breeding efforts, only moderate genetic resistance against FHB exists and the molecular basis of many of the proposed resistance categories remain obscure (Ma et al., 2025). Therefore, improving our understanding of both *F. graminearum* virulence mechanisms and the host traits that limit their effects is essential for application of existing knowledge, identifying new routes to resistance and effectively combating FHB.

1.2 *Fusarium graminearum*: infection strategies and virulence factors

While FHB is caused by several species of *Fusarium* including *F. poae*, *F. avenaceum*, and *F. equiseti*, all with their own unique infection strategies, however, the most prominent causative agent in cereal crops, and the focus of this study, is the *Fusarium graminearum* species (Xue et al., 2019; Chen et al., 2022). *F. graminearum* is considered a highly virulent and adaptable pathogen that can colonize living host tissue but also overwinter on infected crop residues (Moonjely et al., 2023). Under warm-humid conditions, it produces both sexual spores (ascospores) and asexual spores (conidia), which are dispersed via wind, rain splash and through insects to infect plants (Manstretta et al., 2016). Once the spores land on suitable host tissue, they germinate and colonize the host surface (Buttar et al., 2024). The fungus establishes specialized unbranched hyphae called runner hyphae, which facilitate fungal spread across the plant's surface and assist in locating suitable penetration sites such as stomatal openings, wound sites or other weakened areas in the plant cuticle (Niu et al., 2024; Goswami & Kistler, 2004). Following surface colonization, specialized runner hyphae differentiate into multicellular structures known as infection cushions (ICs) (Mentges et al., 2020). These structures generate multiple penetration sites through the plant cuticle, allowing *F. graminearum* to enter the underlying host tissue. During infection, ICs also become sites where genes associated with production of secondary metabolite virulence factors such as DON and fusaoctaxins are upregulated (Mentges et al., 2020). *F. graminearum* produces numerous secondary metabolite virulence factors that contribute to host colonization and disease progression (Gutiérrez-Sánchez et al., 2023). Well-known examples include the previously described trichothecenes DON as well as its acetylated

derivatives 3-ADON and 15-ADON, non-ribosomal peptides such as fusaoctaxins and gramillins and the terpenoid culmorin (Jansen et al., 2005; Jia et al., 2019; Oide & Turgeon, 2020; Brauer et al., 2024 Westphal et al., 2019). The virulence function of DON is associated with promoting fungal spread from infected wheat spikelets into adjacent rachis tissues by limiting callose deposition which is an important defense response in plants whereby they reinforce their physical barriers to restrict pathogen spread (Jansen et al., 2005; Armer et al., 2024; Ellinger & Voigt, 2014). Similarly, fusaoctaxin A has been linked to facilitating cell-to-cell movement of the pathogen by suppressing callose deposition in wheat tissue (Jia et al., 2019). The virulence function of culmorin has been associated with suppressing DON detoxification capacity of host UDP-glycosyltransferase enzymes in wheat (Michlmayr et al., 2026). Gramillins function as cation-conducting ionophores that activate host stress signaling pathways associated with increased susceptibility and enhanced fungal virulence gene expression (Brauer et al., 2024). Evidently, these metabolites can promote fungal virulence by directly interfering with host defenses to promote mycelial growth or by indirectly modifying the effects or accumulation of other virulence factors.

The production of these secondary metabolite virulence factors is a metabolically costly and tightly regulated process (Keller, 2019; Rokas et al., 2020). These compounds are synthesized through the coordinated expression and activity of several proteins encoded by genes within biosynthetic gene clusters (BGCs). For example, a BGC can contain one or more core biosynthetic genes encoding enzymes such as terpene synthases or non-ribosomal peptide synthetases that synthesize the metabolite backbone, alongside genes encoding tailoring enzymes that can modify this backbone or proteins involved in

transporting the biosynthetic product (Hoogendoorn et al., 2018; Rokas et al., 2020). In *F. graminearum*, DON biosynthesis is regulated by the *TRI* gene cluster, culmorin is controlled by the *Clm* cluster, fusaoctaxin biosynthesis involves the *NRPS9* gene cluster and gramillins are produced by the *NRPS8* gene cluster. (Zhou et al., 2021; Wipfler et al., 2019; Westphal et al., 2019, Bahadoor et al., 2018). Furthermore, the expression of specific *F. graminearum* BGCs can be differentially regulated by transcription factors that are expressed under various environmental conditions including pH, oxidative stress and light (Gardiner et al., 2009; Ponts et al., 2007, 2009; Kim et al., 2014). Environmental cues can be sensed by the fungus through specialized transmembrane receptors that activate downstream signaling cascades and alter the activity of transcriptional regulators controlling secondary metabolite biosynthetic genes. For example, extracellular pH is sensed through a transmembrane pH sensor known as PalH which initiates signaling that promotes the cleavage and nuclear localization of a pH-responsive transcription factor Pac1 (Wang et al., 2025). In *F. graminearum*, Pac1 subsequently regulates fungal secondary metabolite production such as the repression of the trichothecene biosynthetic pathway (Merhej et al., 2011). Oxidative stress is an example where the environmental cue itself results in structural changes and nuclear localization of a transcription factor known as FgAP1 that can then induce fungal secondary metabolite gene expression including trichothecene biosynthetic pathway (Merhej et al., 2010, 2011; Montibus et al., 2013; Ponts, 2015). Regulation of DON biosynthesis provides a well-characterized example of both pH and oxidative stress mediated fungal secondary metabolite gene expression in *F. graminearum*. Merhej et al. (2010) showed that extracellular acidification by the pathogen promoted *TRI5* expression

and DON production, while Merhej et al. (2011) identified Pac1 as a pH-responsive transcriptional repressor of the *TRI* pathway. Similarly, Ponts et al. (2007) demonstrated that exogenous treatment with hydrogen peroxide increased *TRI* gene expression and DON accumulation in *F. graminearum* liquid cultures. Montibus et al. (2013) further linked oxidative stress to trichothecene regulation through the transcription factor FgAP1 which is the *F. graminearum* homologue of the yeast bZIP transcription factor Yap1 that regulates genes involved in oxidative stress response such as catalases. Deleting *FgAP1* eliminated the increase in *TRI* gene expression and DON/15-ADON accumulation that was following hydrogen peroxide treatment (Montibus et al., 2013). Together, these findings indicate that secondary metabolite BGC expression in *F. graminearum* is tightly controlled by environmental cues and pathway-specific regulators.

During infection, the host itself represents a complex and dynamic environment. For example, plant responses and pathogen activity can alter apoplastic pH or enhance presence of reactive oxygen species (ROS) encountered by the fungus and such shifts in environmental conditions may influence fungal secondary metabolism (Li et al., 2014; Merhej et al., 2010, 2011; Gu et al., 2022; Ponts, 2015; Montibus et al., 2013). Previously, multiple studies have reported induction of fungal BGCs during plant infection including fungal genes involved in fusaoctaxin, gramillin, DON, and culmorin biosynthesis (Sieber et al., 2014; Boedi et al., 2016; Harris et al., 2016). Boedi et al. (2016) compared *F. graminearum* growth and gene expression in living and dead wheat heads and found greater fungal growth on dead tissue but stronger induction of several secondary-metabolite pathways including trichothecenes and culmorin in living tissue. This study highlights how

fungal secondary metabolism is impacted by active signals from the host environment rather than the host serving simply as a nutrient source. Host dependence was also observed in *F. graminearum* gene expression during infection in maize kernels and wheat and barley spikelets (Harris et al., 2016). Genes associated with DON, culmorin and fusaoctaxin pathways were induced in all three hosts, whereas the gramillin-associated *NRPS8* gene cluster was induced throughout maize infection while only low expression was observed in barley and the initial infection stages of wheat infection. Furthermore, it has been previously established that the gramillin-associated *NRPS8* gene cluster is co-expressed alongside the *TRI* gene cluster which is responsible for DON biosynthesis in *F. graminearum* (Bahadoor et al., 2018). Eliminating gramillin production impacted the expression of the fusaoctaxin A *NRPS9* biosynthetic gene during infection of barley head tissue *F. graminearum* (Brauer et al., 2024). Furthermore, gramillin induced ROS in an ILK1- and RBOHD-dependent manner and promoted *NRPS9* expression during Arabidopsis seedling infection (Brauer et al., 2024). These findings suggest that gramillin might function within a coordinated network involving fungal environmental sensing, host stress responses and fungal secondary-metabolite gene regulation. Overall, these studies demonstrate that fungal BGC expression during infection is both host and tissue dependent.

1.3 Overview of plant stress responses

Plants detect diverse abiotic and biotic stresses to initiate signaling responses that activate defense responses and physiological adaptation to the stressful environment. One well-characterized example of stress sensing pathway in plants involves one form of

microbe recognition. Plasma membrane-embedded receptors known as pattern recognition receptors (PRRs) recognize microbe-associated molecular patterns (MAMPs), which are conserved microbial molecules within a microbial group (Yu et al., 2017; Lu et al., 2022). For example, flg22 is a 22-amino acid peptide derived from a conserved region of bacterial flagella that is recognized by the FLS2 PRR (Yu et al., 2017; Jelenska et al., 2017). Recognition of MAMPs by PRRs triggers the activation of receptor-like cytosolic kinases (RLCKs), initiating a phosphorylation cascade that spreads throughout the cell. For example, BIK1 is an RLCK that initiates signaling cascades by phosphorylating calcium channels, leading to calcium influx into the cell (Figure 1). The rapid influx of calcium ions activates calcium dependent protein kinases (CDPKs) and plays a role in triggering the mitogen activated-protein kinases (MAPK) signaling cascade (Yu et al., 2017). BIK1 dependent phosphorylation of NADPH oxidases like RBOHD leads to a ROS burst in the apoplast (Li et al., 2014). Although other stressors can be detected through different mechanisms, they often converge on shared early signaling events such as ion fluxes, calcium influx, reactive oxygen species (ROS) production and kinase signaling cascades (Boller & Felix, 2009; Waszczak et al., 2018; DeFalco & Zipfel, 2021; Bjornson et al., 2016). This convergence is also reflected in transcriptional reprograming. Bjornson et al. (2021) examined Arabidopsis transcriptional responses to 7 microbe and damage associated patterns as well as abiotic stresses and found differential expression of 970 genes including protein kinases for all stresses (Bjornson et al., 2021). This convergence of stress-induced signaling events is sometimes referred to as the generalized stress response which is a rapid, transient and nonspecific response to diverse environmental stressors.

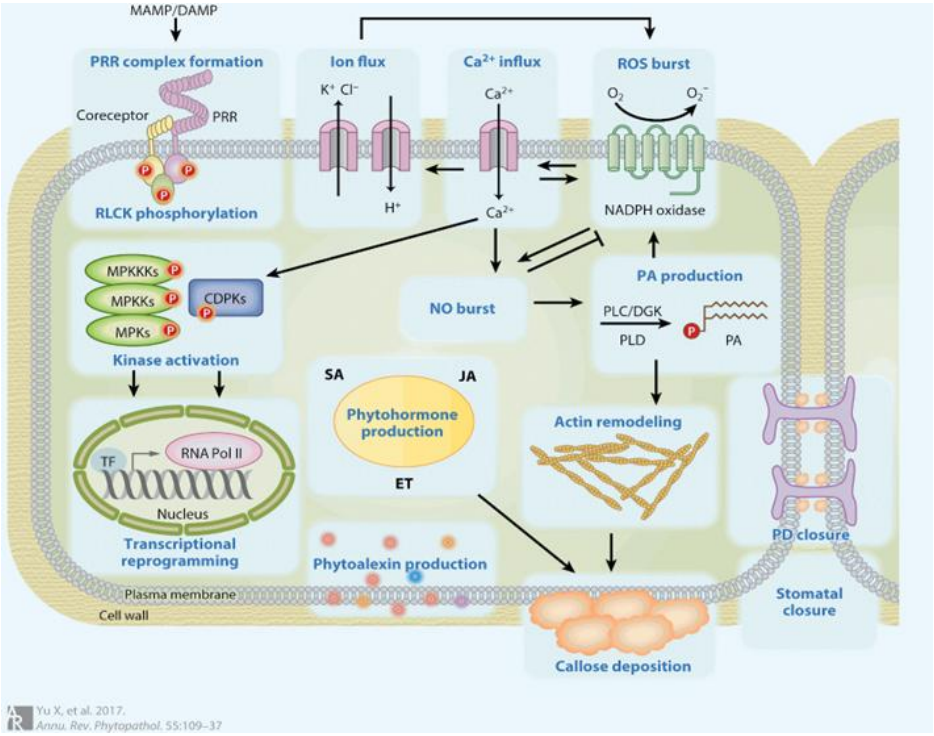

Figure 1: Overview of pattern-triggered defense responses in plants (Yu et al., 2017).

1.4 Ionophores: mode of action, sensing and resistance mechanisms

Ionophores are a diverse group of small amphipathic metabolites that interact with membranes, to induce ion movement across membranes (Ding et al., 2025; Geudens & Martins, 2018). They transport ions across biological membranes through two key mechanisms; by binding specific ions to shield their charge from the hydrophobic membrane interior and releasing the ions on the opposite side or by forming ion-conducting channels in membranes (Balleza et al., 2019). For example, valinomycin and nigericin are described as carrier ionophores, whereas surfactin and leucinostatin A are channel-forming peptides that causes membrane disruption (Huang et al., 2021; Gao et al., 2021; Gilliard et al. 2026; Ishiguro & Arai, 1976). Both mechanisms disrupt cellular electrochemical gradients

required for vital processes such as ATP synthesis, nutrient transport and signaling as well as cell viability (Russell & Houlihan, 2003; Benyamin et al., 2023). Microbes produce ionophores to promote biofilm formation, enable host colonization, to weaken competing microbes or hosts (Raaijmakers et al., 2010). One of the best characterized ionophores that gives insight into both the natural function of these molecules as well as their role in plant-microbe interactions is the cyclic lipopeptide ionophore surfactin, produced by beneficial *Bacillus* species. Surfactin production is stimulated by root-associated cell wall pectin polymers, and it has been shown to promote biofilm formation and tomato root colonization by *Bacillus velezensis* (Hoff et al., 2021). Direct impact against a competing microbe was demonstrated through an *in-vitro* system where *B. subtilis* strains with enhanced surfactin production grow more on LB agar plates as compared to a competing fungal strain *Aspergillus niger* (Richter et al., 2024). In plant-*Bacillus* interactions, the influence of surfactin extends beyond its natural function of improving bacterial fitness and has been linked to activation of induced systemic resistance (ISR) in plants, that enhances host defense against subsequent pathogen invasion (Pršić & Ongena, 2020; Gilliard et al., 2026). Surfactin-mediated ISR has been demonstrated in multiple dicot species, including Arabidopsis, bean, tomato, tobacco and citrus, as well as in monocots such as perennial ryegrass and wheat, against a range of fungal and bacterial pathogens (Ongena et al., 2007; Jourdan et al., 2009; Waewthongrak et al., 2014; Rahman et al., 2015; Le Mire et al., 2018; Gilliard et al., 2026). However, surfactin-induced responses exhibit some concentration dependent host specificity where induction of ISR in dicot roots is observed at low concentrations (5–10 µM) as compared to some monocots like perennial ryegrass (250–500

μM) (Pršić & Ongena, 2020). Recent work has established that surfactin activates ISR through mechanosensing (Gilliard et al., 2026). In Arabidopsis roots, surfactin was shown to preferentially associate with specific membrane sphingolipid - glucosylceramides in the plant plasma membrane. Surfactin inserts its acyl chain into the hydrophobic regions of the target membrane with packing defects acting like a plug. The peptide region of surfactin then interacts with glucosylceramide on the membrane via hydrogen bonds increasing lateral membrane tension and surface rigidity. The size difference between the acyl chain and peptide region of surfactin then induced lipid packing disorder in the hydrophobic core of the membrane (Gilliard et al., 2026). This membrane remodeling activates the host mechanosensitive ion channels MCA1/2 as well as MSL10, resulting in cellular stress responses including transient ion fluxes, membrane depolarization, extracellular alkalinization, calcium influx and intracellular ROS production (Gilliard et al., 2026). Surfactin-treated Arabidopsis plants display stronger subsequent stress response induction to MAMPs such as flg22 and chitin, including enhanced ROS bursts. These plants also displayed reduced infection by *Botrytis cinerea* indicating that surfactin-induced membrane mechanosensing in the plant can prime defense responses and contribute to ISR (Gilliard et al., 2026).

In contrast to surfactin's role in enhancing host resistance, ionophores can also function as phytotoxic virulence factors that promote microbial growth during infection. For example, the cyclic lipopeptide (CLP) gramillin produced by *F. graminearum* is an ionophore virulence factor in maize, Arabidopsis and barley. Gramillin forms cation-conducting pores in plant host membranes causing ion leakage, tissue necrosis and membrane

depolarization (Brauer et al., 2024). Gramillin phytotoxicity exhibits host dependence as well since 3 μM gramillin treatment consistently caused >90% lesioning in dicot species such as Arabidopsis, soybean, canola, tomato and sunflower while monocots such as maize and barley showed >70% necrosis and wheat and sorghum showed <5% necrosis (Brauer et al., 2024). Previous work in Arabidopsis demonstrated that gramillin-induced response involved induction of early generalized plant stress responses including calcium influx, a small transient ROS burst, transcriptional reprogramming, peroxidase activity induction and callose deposition, which is mediated by host stress signaling components BIK1, RBOHD, and ILK1. Furthermore, gramillin sensing was shown to occur independently of canonical MAMP receptors and mechanosensitive ion channels indicating that gramillin and surfactin sensing occurs through distinct mechanisms. Additionally, unlike the protective responses induced by surfactin, gramillin-triggered host stress responses were associated with enhanced disease progression through induction of fungal virulence genes (Brauer et al., 2024). Taken together, these two examples highlight how cyclic lipopeptide ionophores can disrupt plant membranes and activate cellular stress responses, with the resulting effects on defense or susceptibility depending on factors such as host genotype, pathosystem and ionophore concentration.

Resistance to ionophores has been observed across diverse biological systems and can be broadly organized into avoidance, degradation, and recovery mechanisms. Avoidance mechanisms prevent or reduce ionophore access to the membrane. For example, Gram-negative bacteria reduce the ability of ionophores to interact with their membrane through extracellular polysaccharide barriers (Tempelaars et al., 2011; Jenull et

al., 2023; Callaway & Russell 1999; Kevin II et al., 2009). Gram-positive bacteria which lack such intrinsic resistance mechanisms can still acquire ionophore resistance through an adaptive response that involves cell wall thickening (Simjee et al, 2012). Alternatively, degradation mechanisms can directly inactivate ionophores by compromising structural integrity causing insensitivity in the host. For example, resistance to the ionophore daptomycin in *Streptomyces* sp. WAC4713 is mediated by a constitutively produced proteolytic hydrolase, likely a serine protease, that degrades the cyclic ring of daptomycin and generates a linear form that is biologically inactive. This degradation prevented interaction of daptomycin with the bacterial membrane and protected the target organism from membrane depolarization and growth inhibition (D'Costa et al., 2012). Finally, recovery mechanisms restore cellular homeostasis after some ionophore-membrane interactions have occurred. For example, the *NarAB* encodes an ABC transporter in *Enterococcus faecium* which confers reduced susceptibility to ionophores including narasin, salinomycin, and maduramicin by exporting the ionophore (Naemi et al., 2020). Similarly, *TnrB2/TnrB3* also encode ABC transporters in *Streptomyces longisporoflavus* and confer resistance to tetronasin ionophore (Linton et al., 1994). Overall, these examples demonstrate that ionophore resistance can arise through cellular traits that prevent ionophore-membrane interactions, utilize enzymatic activity to degrade the ionophore or rapidly recovery from ionophore mediated membrane disruption.

1.5 Gramillin sensitivity in barley and its impact on *F. graminearum* gene expression

Gramillin is a CLP ionophore produced by *F. graminearum* that is essential for full pathogen virulence in maize, barley and Arabidopsis but not in wheat. Gramillin can

integrate into susceptible host plasma membranes and disrupt ion homeostasis, resulting in uncontrolled ion leakage and necrotic tissue collapse within hours of treatment (Brauer et al., 2024). Sensitivity to this toxin is characterized through ion-leakage measurements and the observation of necrotic lesion formation on host tissue. Lesion formation was associated with enhanced fluid accumulation in the apoplast and is influenced by environmental humidity, where an increase in environmental humidity lowers lesion severity (Brauer et al., 2024). Gramillin sensitivity is independent of active plant metabolism, since inhibitors of ROS production, electron transport and photosynthesis did not block gramillin-induced necrosis. Lanthanum chloride treatment partially reduced necrosis, suggesting that cation-binding can modify gramillin activity however, calcium chelators like EGTA did not provide protection indicating that calcium-dependent signaling is likely not necessary for gramillin toxicity (Brauer et al., 2024). Furthermore, gramillin sensitivity was higher in *bik1, rbohD* and *ilk1* knockout mutants indicating that inducible stress responses are not necessary for gramillin induced phytotoxicity.

Among cereal hosts, gramillin toxicity is host-specific since purified gramillin A and B induced ion leakage and tissue necrosis in maize and barley but not in wheat (Brauer et al., 2024). A range of sensitivities to gramillin toxicity was also observed among barley genotypes, as measured by differences in gramillin induced ion leakage and lesion severity (Power, 2023). Notably, the Lowe barley genotype is insensitive to gramillin compared with sensitive genotypes such as Leo, Radegast, and AAC Connect, although the physiological basis of this insensitivity remains unresolved (Power, 2023). The gramillin insensitivity in Lowe has been mapped to a major quantitative trait locus (QTL) on the 5H chromosome

(unpublished data). Developing molecular diagnostic tools that can track this gramillin sensitivity in barley genotypes would be a valuable tool for incorporating gramillin insensitivity from Lowe into new varieties. Furthermore, investigating genes localized in this region could also provide insight into traits that potentially influence gramillin sensitivity in barley. The observed differential sensitivity to gramillin in barley genotypes could arise through different ionophore resistance mechanisms. Host membrane properties may reduce the ability of gramillin to reach or interact with the plasma membrane, representing a form of avoidance. Alternatively, the host may enzymatically degrade gramillin before any extensive membrane disruption occurs. Finally, insensitivity may be a recovery mechanism that is dependent on differential gramillin-induced membrane disruption and stress responses.

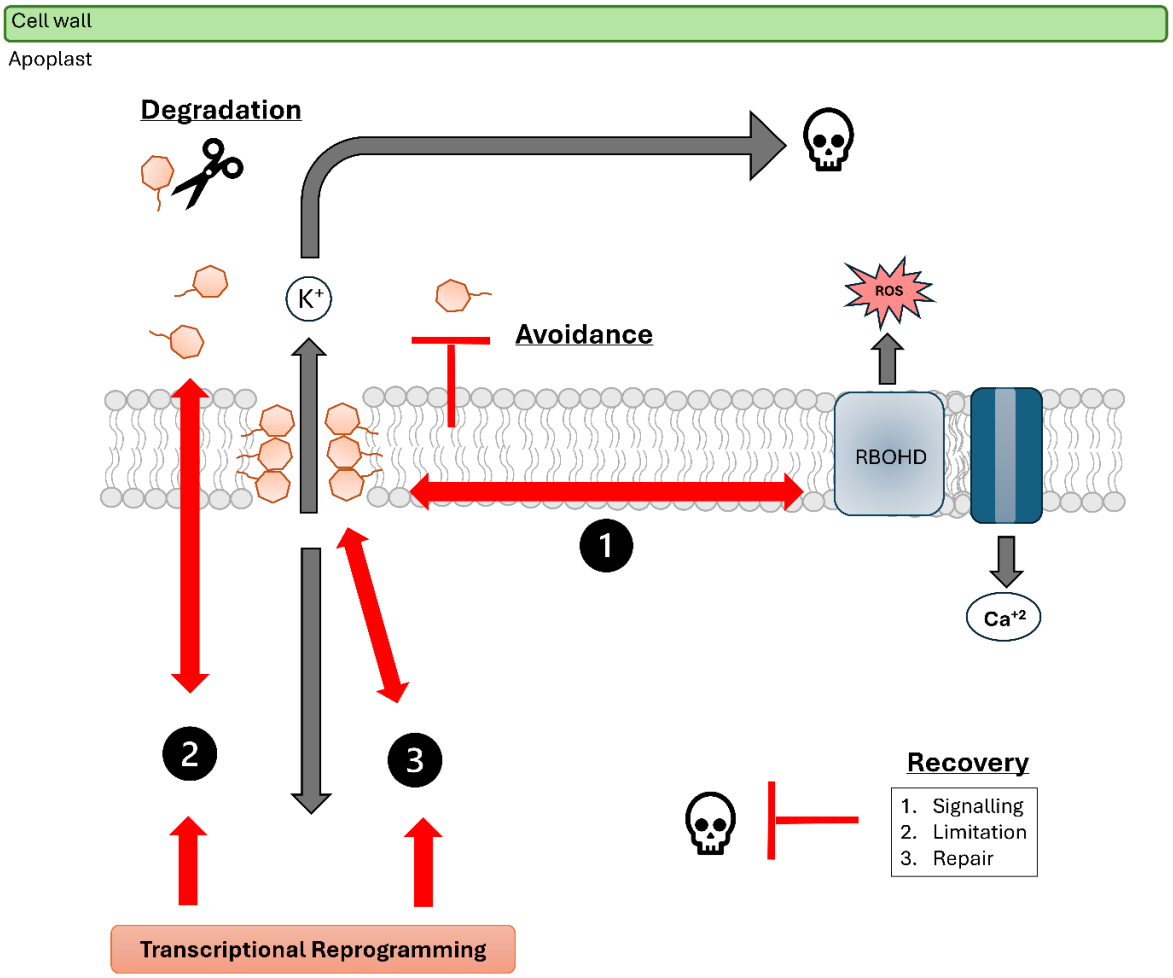

Figure 2: A working model summarizing potential mechanisms underlying gramillin insensitivity in Lowe barley. We hypothesize that gramillin insensitivity may arise from the three broad categories of known ionophore resistance mechanisms; **Avoidance** suggests innate differences in membrane properties prevent any gramillin interaction with Lowe's membrane. **Degradation** predicts constitutive or induced host enzymes break down and inactivate gramillin differentially in Lowe. **Recovery** proposes that gramillin interacts with membrane but Lowe is able to prevent the phytotoxic effects through 1) altered gramillin-induced signaling, 2) rapidly limiting gramillin-induced membrane damage and 3) rapid

membrane repair. (Red arrows indicate hypothesized mechanisms; Skulls indicate cell death).

In addition to directly damaging host membranes, gramillin may indirectly influence *F. graminearum* gene expression by altering environment conditions sensed by the fungus during infection. Arabidopsis seedling infection assays showed that knockout of *ilk1* or *rbohD* reduced susceptibility to *F. graminearum*, indicating that these host genes promote to disease susceptibility. Expression of the fusaoctaxin biosynthetic gene *NRPS9* was reduced in the absence of gramillin production and during infection of the *rbohD* and *ilk1* knockout mutants, whereas expression of the trichothecene biosynthetic gene *TRI5* was unaffected. A similar trend was observed in barley spikelet tissue where, *NRPS9* expression was impacted by gramillin production but not *TRI5*. Hence, there is a link between gramillin induced host responses and induction of fungal virulence genes. However, it is unclear whether natural differences in gramillin sensitivity among barley genotypes can also impact the expression of fungal virulence genes during infection. Comparing gramillin sensitive and insensitive barley genotypes will provide an opportunity to determine link between these two factors as well.

1.6 Research Objectives

To understand the physiological basis of gramillin insensitivity in Lowe and its impact on fungal expression during infection, I put forth three research objectives that will be addressed throughout this study;

1. Generate tools to track gramillin insensitivity in barley genotypes.

2. Characterize the gramillin insensitivity in Lowe barley by gathering evidence on avoidance, degradation or recovery mechanisms relative to gramillin-sensitive genotypes.

3. Evaluate the impact of gramillin and host sensitivity on fungal secondary metabolite biosynthesis during barley infection.

2. Methods

2.1 Plant material

All plants were grown in growth chambers (Conviron CMP3244) set at 21ºC and approximately 50% humidity with 16 hours of daylight (300 µmol/m^2/s). Barley was grown in soil (75 PROmix BX:24 black earth:1 lime) with 1-2 seeds per pot in a 32-pot insert per tray and watered daily. The barley genotypes used include Lowe, AAC Connect, Leo and Radegast which are all 2-row spring barley varieties primarily used for malting (Juskiw et al., 2019, Government of Canada – Canadian food inspection agency, 2022; Beratto, 1990; Svacina, 2005).

2.2 Gramillin purification and quantification

Gramillin purification was conducted by Dr. Indira Thapa using previously established protocol (Bahadoor et al., 2018). A purified mixture of gramillin A and B (approximately 50:50 ratio of A and B) was used for all assays and the concentration of cyclic gramillin was verified using HPLC by Dr. Indira Thapa for every batch of resuspended gramillin.

To evaluate gramillin degradation, apoplastic fluid was isolated from 3 week-old AAC Connect and Lowe barley using a method adapted from B.M. O'Leary et al. (2014) to isolate the apoplastic fluid. However, proteomics revealed that the extract contained both apoplastic and intracellular proteins and thus is not a pure apoplastic fluid. Leaves from 3 week-old barley plants were collected and cut into 6 cm sections. The leaves were then washed and blot dried using a Kim wipe. The dried sections were then stacked on a three pronged screen mesh that was placed inside a 50ml falcon tube. The set up was then centrifuged at 3110 rpm for 20 minutes at 20 °C. The extract is transferred to a new 1.5 mL centrifuge tube for use immediately or flash frozen and stored at –80 °C. The extract was split into two aliquots; one was boiled at 90 °C for 10 minutes, and the other was kept untreated on ice. One non-extract water control, the boiled and the unboiled apoplastic fluid samples were then incubated with 40 µM purified gramillin, for 30 minutes at room temperature, after which gramillin concentrations were quantified using UPLC-HRMS. For each replicate sample of apoplastic fluid, leaves were taken from 5-6 barley seedlings per genotype and pooled together. The gramillin degradation assay was repeated twice with 3-4 apoplastic fluid samples per genotype. The proteomics analysis was conducted once using 3 apoplastic fluid samples per genotype.

2.3 Protein identification

The barley apoplastic fluid described above were also tested to identify proteins within the extracts. Apoplastic fluid was isolated from 5-6 three-week-old Lowe or AAC Connect plants to generate a replicate, and three independent replicates were evaluated per

genotype. The extracts were flash-frozen in liquid nitrogen and shipped to the University of Guelph for proteomic analysis. The proteomics dataset was generated by Dr. Jason McAlister of the Geddes-McAlister Lab. Mass spectrometry data was processed using Spectronaut (DIA workflow), and proteins were annotated against the *Hordeum vulgare* UniProt reference proteome (UP000011116; 35,907 protein entries; downloaded October 28, 2025). Statistical analysis was performed using Perseus v1.6.2.2 and protein abundance values were log2-transformed. Within the dataset, the criteria for genotype specific enrichment of proteins was the absolute difference in average log2 intensity between Lowe and AAC Connect > 2. Protein localization was determined based on Gene Ontology annotations within the cellular component category.

2.4 KASP genotyping

KASP markers were developed by Dr. Micheal Holtz using Kraken™ (LGC Biosearch Technologies) software by the Western Innovations Corp (Supplemental Table 1). The KASP primer master mix comprised 30 µM of the common reverse primer and 12 µM of each forward primer. Genomic DNA from selected 2-week-old barley cultivars was extracted using the Phytopure DNA Extraction Kit (Cytiva, RPN8511) as per the manufacturer's instructions. The assay was conducted in the FrameStar® 96 Well Skirted black well, black frame PCR Plate (Thomas Scientific, 1149V66) and reaction mixture was 10 µL total volume (including 5 µl of 2xPACE 2.0 Genotyping Master Mix (3CR Bioscience, 003-0001), 0.14 µl of KASP primers master mix, 5 µl of genomic DNA (~22ng)). The PCR plate was run with an initial hot-start activation of 15 min at 94°C, followed by 10 touchdown cycles (94°C for 20 s,

touchdown at 65°C initially and decreasing by 0.6°C per cycle for 60 s), and 26 additional cycles of annealing and extension (94°C for 20 s, 55°C for 60 s). Data analysis and visualization was done using KlusterCaller software. The assay was repeated 2-3 times depending on the genotype with the same results.

2.5 Leaf drying assay

Leaf sections (5 cm) from 2 week-old Lowe and AAC Connect barley plants were infiltrated with water or 10 µM gramillin and weighed. The sections were then allowed to stand vertically in a stand at room temperature for 2 hours after which they were weighed again. The weight after 2 hours was subtracted from the initial weight of a leaf section to calculate water loss. Five leaf sections per genotype were used and the experiment was repeated 3 times with similar results.

2.6 Lesion assay

The first leaf of a two- to three-week-old barley seedling was syringe-infiltrated with a 5-20 µM purified gramillin as indicated, or water as a control. The infiltrated area was circled, and the seedlings were returned to their growth cabinet for 24 hours, until the area was scored. A score of 0 indicates no lesioning; 1 indicates 1-25% of the infiltrated area has lesioned; 2 indicates 26-50% lesioned; 3 indicates 51-75% lesioned; and 4 indicates 76-100% lesioned (Bahadoor et al., 2018, Brauer et al., 2024). For chemical inhibitor studies, 2 mM salicylhydroxamic acid (SHAM) (Sigma-Aldrich, S607), 25 µM diphenyleneiodonium (DPI) (Sigma-Aldrich, D2926) and 1mM EGTA (Sigma-Aldrich, E3889) were mixed with 20 µM

purified gramillin and co-infiltrated. For flg22 pre-treatment study, the gramillin treated section of the leaf was infiltrated with 1 µM flg22 or water, 24 hours prior to 10 µM gramillin treatment.

2.7 Ion leakage Measurements

The first and second fully expanded true leaves of two- to three-week-old barley seedlings were used to measure conductivity as a proxy for ion leakage as described in Bosnich et al. (2025). Three barley leaf disks (4 mm) from Lowe and AAC Connect genotypes were submerged in 200 µl of toxins in a 96-well plate. The toxins used in this study include – 50 µM Ionomycin (Sigma-Aldrich, I0634), 500 µM Surfactin (Sigma-Aldrich, S3523), 50 µM Nigericin (Sigma-Aldrich, N7143) and 20 µM Leucinostatin A (Cayman Chemical, P168). The plate was then placed in a bell jar with a vacuum nozzle and hose attached. The vacuum pressure was turned on until the vacuum reached 9.8 pounds/square inch (approximately 10 seconds). This process was repeated 6 times. A lid was added to the plate and incubated on an orbital shaker (55rpm) under light (13 W, 50 µmol·m-2·s-1) placed 23 cm above the shaker for 24 hours. The ion conductivity was then measured using the COND-905 micro conductivity probe (Lazar Research Laboratories Inc.) which was fully immersed in the liquid in each well. The probe was washed with Milli-Q water and dried using a Kimwipe before each measurement. The instrument was calibrated according to the manufacturer's instructions, and the conductivity of Milli-Q water was noted as a baseline reference. For each independent trial, 4 barley seedlings were used per genotype and treatment. The experiment was repeated 3 times with similar results.

2.8 RNA extraction and qRT-PCR

To monitor the effect of gramillin on barley gene expression, the first leaf of 3 week-old Lowe, Leo, AAC Connect and Radegast barley plants were infiltrated with 5 µM gramillin or H_2O using a needleless syringe. Leaf tissue was harvested 4 hours post-infiltration and immediately frozen in liquid nitrogen. For each independent trial, 4 barley seedlings per genotype per treatment. The experiment was conducted 3 times with similar results. For infected barley leaf disks, samples were harvested 3 days post inoculation and flash frozen in liquid nitrogen. The samples comprised of both the infected leaf disk and any leftover inoculation liquid in the well. The experiment was conducted 3 times with similar results. In one experiment, infected leaf disks were collected from 6 wells and was pooled for RNA extraction. In the other two experiments, infected leaf disks were collected from 12 wells, pooled and ground together for RNA and metabolite extraction with approximately half of the ground sample being used for RNA extraction.

The RNA was extracted using the QIAGEN RNeasy Plant Mini Kit (QIAGEN, 74106). RNA was reverse transcribed using the Applied Biosystems cDNA synthesis kit according to the manufacturer's instructions (Applied Biosystems, 4374967). For each qPCR reaction, the PowerUp SYBR Green Master Mix (Applied Biosystems, A25742) was used with a final reaction volume of 10 µL containing 0.5 µM of each primer and 1 µL of cDNA (Supplemental Table 3). The amplification conditions consisted of an initial denaturation at 95°C for 15 seconds, annealing at 60°C for 15 seconds, and extension at 72°C for 1 minute, and repeated for 40 cycles. Barley gene expression was normalized using the reference genes *HvActin* and

HvCyclophilin (Gines et al., 2018, Burton et al., 2004) and fungal gene expression was normalized using fungal reference genes *Fg GAPDH* (*FGSG_16627*) and *Fg β-tubulin* (*FGSG_09530*) (Harris et al., 2016). The relative expression was calculated using the Pfaffl method (Pfaffl, 2001). Water treated Lowe samples were used as the control condition for gramillin induced barley gene expression calculations and AAC Connect leaf disks infected by a transformation control fungal strain (Bahadoor et al., 2018) was used as the control condition for infection assay fungal gene expression calculations.

2.9 RNA-seq analysis

A transcriptional profiling experiment capturing the impact of flg22 and gramillin in Lowe and Leo barley was generated previously (Brauer et al., 2025). Genes were deemed differentially expressed (DEGs) if they had a False Discovery Rate (FDR) of less than 0.05 and a log2 fold change greater than 1 when compared to a water control. In this work, the DEGs were evaluated for gene ontology enrichment analysis using g:Profiler and default settings (Kolberg et al. 2023). Venn diagram analysis was conducted using Venny 2.1.

2.10 Callose quantification

Callose deposits were counted using methods described previously in S. Schenk et al. (2015). Two- to three-week-old barley leaves were infiltrated with 5 µM gramillin or water and after 24 hrs, three leaf disks (4mm) were taken per infiltrated leaf. The leaf disks were fixed in 1:3 acetic acid: ethanol until they were transparent for 30-35 hrs. The leaves were then incubated for at least 4 hrs in a staining solution (150 mM K_2HPO_4 and 0.01% (w/v)

aniline blue (Sigma-Aldrich, 415049). The leaves were embedded in 50% glycerol (Thermo Fisher Scientific, G33) and callose deposits were counted manually under a fluorescence microscope (Leica Zeiss) using a DAPI filter at 20x magnification. For each independent trial, 10 leaf disks collected from 3 different plants samples were counted per genotype and treatment. The experiment was repeated 3 times with similar results.

2.11 Fungal culturing and infection assay

The *F. graminearum Δgra1-1* mutant and transformation control strains were used for experimentation (Bahadoor et al. 2018). The strains were revived from -80°C glycerol stocks (15%) and cultured on synthetic nutrient agar (SNA) medium plates at 25°C in dark for 5 days to induce sporulation and stored at 4°C for up to 2 weeks (Bahadoor et al. 2018). To prepare conidiophores for the *in vitro* inoculation assays, six 3 mm plugs were extracted from the SNA plate and transferred to 50 mL of SN medium in 250 mL Erlenmeyer flask. Cultures were incubated at 28°C with shaking at 170 rpms for 3 days in dark to generate conidiophores. Four layers of sterile cheesecloth were used to separate mycelial solids from conidia. Spores were washed with sterile water twice by centrifugation at 4200 rpms for 10 minutes at 4°C. Pelleted spores were resuspended in 20 mL sterile water and quantified with a hemocytometer under an optical microscope (Leica DMLB). The isolate fungal spores are resuspended in 10 mL of 0.5% sucrose at a final concentration of 800 spores/mL.

To inoculate barley leaf disks, 50 µL of the spore suspension is pipetted in to each well of a 96-well plate (Grenier transparent, flat bottom). One 4mm diameter leaf disk from 2-3 week old barley was added to each well. The plates were sealed with Micropore tape and

placed in a growth chamber at 21°C with 16h daylight for 3 days until harvesting for RNA and metabolite extraction. For each replicate, infected leaf disk tissue was harvested at 3 dpi from 12 wells, with each well containing one leaf disk and pooled together as one sample. For metabolomics only, 6 uninfected leaf disks per genotype were included as a negative control. The pooled tissue was immediately flash frozen in liquid nitrogen and ground to a fine powder using a mortar and pestle. The ground tissue was then divided into two approximately equal portions for paired fungal gene expression and metabolomic analysis. One half of the ground tissue was used for RNA extraction and downstream qPCR analysis. For each independent trial, leaf disks were collected from 16-20 individual barley seedlings per genotype. Samples were distributed across five replicate 96-well plates. The experiment was conducted 2 times with similar results.

2.12 Metabolomics

Ground, infected leaf disk tissue was weighed and transferred into reinforced 2 ml tubes (VWR International, Ltd, 10158-556) and flash frozen using liquid nitrogen. Metabolites were extracted by adding 300 µL acetonitrile containing 0.1% formic acid and gently mixing on an oscillating flat rotary mixer (Clay Adams, 1105) for 2 hours at 60 rpm. Extracts were then centrifuged at 15,000 rpm for 8 minutes to pellet debris, and 150 µL of clear supernatant was transferred into labeled 2 mL Virtuoso SureStop amber vials (Thermo scientific, 6ASV9-2P) and sent for metabolomic analysis using UPLC-HRMS to the Overy Lab. The downstream metabolomic profiling was conducted using mzMine software and the general methodology has been adapted from Eranthodi et al., 2020.

3. Results

3.1 Gramillin insensitivity in Lowe is toxin-specific and associated with a region on chromosome 5H

To determine if Lowe's ionophore insensitivity extended beyond gramillin we compared Lowe and AAC Connect leaf responses to ionomycin, surfactin, nigericin and leucinostatin A ionophores. All ionophores induced ion leakage relative to water in both genotypes to a similar extent, indicating Lowe's insensitivity is not explained by broad spectrum tolerance to ion imbalance or membrane disruption (Figure 3A).

A major QTL on chromosome 5H underlying gramillin induced ion leakage was identified in two independent mapping populations generated from crosses between Lowe and either gramillin-sensitive AAC Connect or Radegast genotypes (unpublished data). To track Lowe-derived gramillin insensitivity, KASP markers (K1, K2) were developed and tested on genotyped lines from the two populations (Table 1). The KASP genotyping results matched the sequencing-based genotyping in 19 out of 20 genotypes for the K1 marker (based on the S5H_2645485 SNP) and 10 out of 12 genotypes for the K2 marker (based on the S5H_2468415 SNP) (Table 2) confirming primer effectiveness. Lowe was developed from a cross between Ponoka and the breeding line H92017203Z which originates from a cross between AC Oxbow and Leo (Juskiw et al., 2019). Previous ion-leakage measurements indicate that Ponoka, AC Oxbow and Leo are all gramillin-sensitive varieties (Power, 2023). KASP genotyping of parental lines indicate that Ponoka and Leo carry the gramillin insensitivity alleles, whereas AC Oxbow carries the gramillin sensitivity allele (Figure 3B).

Overall, these results highlight Lowe's insensitivity phenotype is specific to gramillin and that KASP primers can be used to track the insensitivity alleles.

3.2 Gramillin degradation is similar between gramillin-sensitive and -insensitive genotypes

To understand what traits are associated with gramillin insensitivity in Lowe, we hypothesized that Lowe may be degrading gramillin more than sensitive genotypes. To test this, we extracted plant fluids from AAC Connect and Lowe leaves. The pH of the fluids was 5.8-6.2 with no significant difference between genotypes (Figure 4A). Plant extracts degraded gramillin in both genotypes to a similar extent and boiling the extracts eliminated the degradation activity in both genotypes (Figure 4B). Predicted gramillin degradation products accumulated in the unboiled extracts confirming digestion of the peptide (Figure 3D). The cleavage appears to occur at the amide bonds in these predicted degradation products which is common site of action for proteases (Mahesh et al., 2018).

To determine which proteins with potential peptide degrading activity were present in the extracts, proteomic analysis of the extracts was conducted. Signals from 2,128 unique proteins from apoplastic, membrane and intracellular locations were identified where 2,047 were detected in both genotypes (Supplemental Data 1A). The remaining 48 were more abundant in AAC Connect samples and 33 were more abundant in Lowe samples (Figure 4C). Among the 214 predicted apoplast-localized proteins, we identified 14 proteins with predicted roles in proteolysis (GO:0051603, GO:0006508) based on gene ontology the majority of which were found in both genotypes (Supplemental Data 1A, B).

Together, these results suggest that barley leaf fluid contains heat-sensitive enzymatic activity capable of degrading gramillin. However, this degradation activity was

observed to a similar extent in both genotypes, suggesting that it is unlikely to account for Lowe-specific gramillin insensitivity.

3.3 Gramillin induces attenuated stress responses in Lowe

Gramillin induced lesioning can be reversed in Arabidopsis leaves by applying high humidity suggesting that gramillin toxicity is linked to leaf drying (Brauer et al., 2024). To determine if Lowe insensitivity is due to physiological differences that influence leaf drying rates, we tested water loss in Lowe and AAC Connect leaves after infiltration with water or gramillin. No differences in drying rates were observed between genotypes (Figure 5A). Next, we hypothesized that gramillin may induce different cellular responses in sensitive and insensitive barley. In particular, if induced cellular stress responses are required for gramillin insensitivity in Lowe, Lowe may exhibit higher inducible stress responses than AAC Connect. On average, gramillin induced a ~56 fold increase in callose deposition relative to the water control in the gramillin sensitive barley genotypes as compared with a ~22 fold increase in Lowe (Figure 5B). Although Lowe showed a significant induction of callose deposition, the magnitude of induction was ~2.5 fold lower than the average response observed in the gramillin-sensitive genotypes.

Transcriptomic profiling of gramillin-treated leaves similarly revealed a prolonged transcriptional response in gramillin-sensitive Leo compared to the insensitive Lowe genotype (Figure 5C). In Leo, gramillin altered expression of 1323 genes at 30 minutes and 3885 genes at 4 hours relative to the water control. In contrast, Lowe had a strong transcriptional response at 30 minutes with 2120 differentially expressed genes (DEGs), followed by fewer genes affected at 4 hours (1175) (Figure 5C, Supplemental 2A-D). At both

timepoints, just over 20% of DEGs were shared between genotypes which were enriched in glycosyltransferases and amino acid metabolism at 30 minutes and protein kinases at 4 hours (Figure 5C, Supplemental Data 3A and 3B). At 30 minutes, both Lowe and Leo-specific DEGs are enriched in genes that encode enzymes involved in signal transduction; however, Lowe was uniquely downregulating glutathione-associated metabolism genes (Figure 5D, Supplemental Data 3C and 3D). In contrast, at 4 hours the genes that were upregulated in Lowe were enriched in genes with a putative role in carbohydrate metabolism (Supplemental Data 3E).

Within the gramillin sensitivity QTL region, two genes showed differential transcriptional responses to gramillin treatment. A putative glycosyltransferase gene was upregulated in both genotypes, with a stronger induction in Lowe, whereas a gene encoding an elongation of fatty acids protein 3-like (ELO) protein, which is associated with membrane lipid biosynthesis, was downregulated in Lowe but remained unchanged in Leo (Supplemental Data 2J).

At 4 hours, DEGs that were upregulated in Leo, but not Lowe were significantly enriched in genes with potential roles in signal transduction, vesicle transport, and defense suggesting a sustained induction of stress responses (Supplemental Data 2D). To validate this observation in two other gramillin-sensitive barley genotypes (AAC Connect and Radegast), we tested expression of two gramillin responsive genes that are induced in Leo but not in Lowe after 4 hours using quantitative PCR. These genes were also found to be defense marker genes in barley previously (Brauer et al., 2025). Gramillin induced *WRKY23* expression by approximately 3.2 and 2.0 fold and *NBS-LRR* expression by

approximately 7.9 and 2.3 fold relative to the water controls in AAC Connect and Radegast, respectively, while no induction was observed in Lowe (Figure 5E). Together, these results indicate that gramillin induces callose deposition and transcriptional reprogramming in Lowe and gramillin-sensitive genotypes, but the responses are more transient in Lowe as compared to gramillin-sensitive genotypes.

3.4 Inducible stress responses are intact in Lowe barley and are dispensable for gramillin phytotoxicity

To determine if Lowe produces typical stress responses relative to gramillin-sensitive barley genotypes, we treated leaves with the flg22 MAMP which induces ROS production, callose production and transcriptional reprogramming in barley (Brauer et al., 2025). The flg22 peptide induced similar apoplastic ROS bursts in Lowe, Leo, Radegast and AAC Connect (Figure 6A). Transcriptional profiling also revealed a similar number of DEGs induced by flg22 relative to the control treatment in Lowe (696 at 30 minutes and 2,094 at 4 hours) and Leo (767 at 30 minutes and 1,712 at 4 hours) (Figure 6B, Supplemental Data 2E-H). Shared DEGs between genotypes reached a maximum at 4 hours with 1163 DEGs which are enriched in genes encoding for protein kinase activity and defense response-associated genes (Figure 6B, Supplemental Data 3F). Approximately 44% of flg22-induced genes are shared between both genotypes as compared to an overlap of only 23% of the gramillin induced genes between both genotypes at 4 hours (Figure 7A). This indicates that Lowe and Leo exhibit more similar transcriptional responses to flg22 than to gramillin treatment. Together, these results suggest that Lowe barley has intact inducible stress response

capacity and that its transient response to gramillin is unlikely a result of general defect in stress signalling capacity. Interestingly, there are 389 DEGs shared between both genotypes and treatments which are enriched in upregulated genes that encode proteins kinases and downregulated genes that encode putative glucosidases and may represent important general stress response marker genes in barley (Figure 7 A, B).

To determine if inducible stress responses influence gramillin sensitivity, chemical inhibitors of peroxidase activity, NADPH oxidase activity and calcium transport were applied alongside gramillin to barley leaves. None of the inhibitors impacted gramillin induced necrosis in AAC Connect or gramillin insensitivity in Lowe suggesting that inducible stress signaling is dispensable for gramillin phytotoxicity (Figure 8A). Next, barley leaves were pre-treated with flg22 prior to gramillin infiltration. The MAMP pre-treatment reduced gramillin-induced lesion severity by 32% in AAC Connect and had no effect in Lowe suggesting a minor impact of flg22-induced responses on gramillin phytotoxicity (Figure 8B).

3.5 Gramillin and its impact on the host fungal secondary metabolite expression during infection

Previous studies show that gramillin production is required for full expression of *NRPS9* during barley infection (Brauer et al., 2024). To determine if this associated is based on host response to gramillin, we investigated fungal expression of genes involved in secondary metabolite biosynthetic pathways during barley leaf infection in Lowe and AAC Connect barley genotypes using the *Δgra1-1 F. graminearum* mutant strain which lacks gramillin production (Bahadoor et al., 2018). At 3 days after infection, the fungus penetrated

leaf tissue through the stomata and mycelial growth within the leaf disk was observed (Figure 9A).

Within this leaf-disk infection system, we first confirmed expression of the *NRPS8* biosynthetic gene involved in gramillin production in the transformation control (TC) strain and the lack of *NRPS8* expression in the *Δgra1-1* strain (Figure 9B). In the gramillin-sensitive AAC Connect, *TRI3, TRI9* and *Clm1* expression was significantly reduced by 72.9%, 50.7% and 76.5%, respectively, following infection with the *Δgra1-1* strain compared with the TC strain (Figure 9B). Compared with AAC Connect infected with the TC strain, *TRI3* and *Clm1* expression was significantly reduced by 54.5% and 73.6%, respectively, in Lowe infected with the TC strain (Figure 9B), while *TRI9* expression was 36.3% lower, it did not differ significantly ($p = 0.0899$). Similarly, comparing AAC Connect infected with the TC strain with Lowe infected with the *Δgra1-1* strain, *TRI3, TRI9* and *Clm1* expression was 85.2%, 65.6% and 90.8% significantly lower respectively (Figure 9B). Interestingly, fusaoctaxin biosynthetic genes (*NRPS9, Fgm5*) did not exhibit similar trends as they were expressed similarly across both genotypes and strains. No differences in secondary metabolite accumulation were observed between genotypes or strains (Figure 10).

4. Discussion

In this study, we investigated the genetic and physiological basis of gramillin insensitivity in Lowe barley. Collectively, our findings indicate that gramillin insensitivity in Lowe barley is associated with lower gramillin-induced callose deposition and

transcriptional response as compared to gramillin-sensitive barley. Furthermore, we also present evidence that gramillin production and host sensitivity to gramillin were associated with an earlier or stronger induction of fungal virulence gene expression involved in production of trichothecenes and culmorin during barley leaf infection. This aligns with previous work where eliminating gramillin production by the fungus, and host genotypes with reduced gramillin-induced responses showcased lower fungal virulence gene expression during infection (Brauer et al., 2024).

4.1 Gramillin insensitivity is not explained by complete avoidance mechanisms

Insensitivity to ionophores can arise from avoidance mechanisms that interfere with ionophore-membrane interactions. For example, in *Escherichia coli*, the presence of a lipopolysaccharide (LPS) containing outer membrane likely confers resistance against valinomycin, K+ mobile carrier cyclic depsipeptide ionophore, as it restricts inner membrane interactions (Tempelaars et al., 2011). Disruption of the LPS layer using polymyxin B resulted in a 50-fold increase in sensitivity of *E. coli* to valinomycin supporting the role of LPS layer as an avoidance mechanism of ionophore insensitivity (Alatossava et al., 1984). In gram-negative bacteria *Selenomonas ruminantium*, insensitivity to monensin, a carboxylic polyether ionophore, was intrinsic and has also been associated with the presence of an outer membrane layer (Callaway et al., 1999). Interestingly, the gram-positive bacteria *Enterococcus faecium* can acquire reversible monensin insensitivity by thickening its cell wall or glycocalyx following exposure (Simjee et al., 2012). In this study, no genotypic differences in ion-leakage induced by a panel of chemically diverse ionophores was observed between gramillin-sensitive AAC Connect and Lowe barley. The ionophores tested

included carboxylic polyether ionophores nigericin and ionomycin which act as mobile ion carriers, linear peptide ionophores such as leucinostatin A which forms ion conducting channels in the target membrane and the CLP ionophore surfactin (Frederiksen et al., 2024; Taylor et al., 1993; Ishiguro & Arai, 1976; Gilliard et al., 2026). Since Lowe exhibited similar sensitivity as AAC Connect to all the tested ionophores, it suggests that Lowe-specific gramillin ionophore insensitivity is likely not due to broad physiological traits that can limit all ionophore-membrane interactions.

Previous work also indicates that gramillin induced lesion formation is reduced under high humidity conditions (Brauer et al., 2024). Some fungal toxins such as fusicoccin, constitutively activate the plasma-membrane proton pumps, causing irreversible stomatal opening, increased water loss and visible lesion development (Marra et al., 2021). In comparison, gramillin treatment did not increase leaf drying rates, and Lowe and sensitive barley genotypes exhibited comparable water loss. Hence, gramillin likely does not interfere with broad physiological traits such as stomatal regulation to cause sensitivity either. Together, these results suggest that Lowe insensitivity is likely not due to complete avoidance of gramillin- host membrane interactions.

4.2 Gramillin degradation can occur in barley apoplastic fluid but is not Lowe-specific

Enzymatic degradation also represents a potential resistance mechanism against ionophore action as it can disrupt key structural features required for their bioactivity. We observed gramillin degradation product accumulation following incubation in barley leaf fluid from Lowe and sensitive genotype. The predicted gramillin degradation products

suggest the cleavage of an amide bond that results in linearization of gramillin's structure. Previous work has shown that the cyclic structure of gramillin is required for its phytotoxic effects (Bahadoor et al., 2018; Brauer et al., 2024). Ionophore resistance through degradation mechanisms have been observed previously during antagonistic competition between microbes. For example, *Streptomyces* sp. Mg1 is resistant to growth inhibition by surfactin when it secretes the hydrolase SfhA which breaks the ester bonds and linearizes surfactin. Furthermore, deletion of *sfhA* encoding for this enzyme reduced *Streptomyces* growth and made it sensitive to surfactin, directly linking ionophore degradation as a resistance mechanism (Hoefler et al., 2012). Similarly, *Streptomyces* sp. WAC4713 bacteria is resistant to growth inhibition when treated with the antimicrobial cyclic lipopeptide daptomycin (D'Costa et al., 2012). The resistance mechanism was associated with a constitutively active protease-like enzyme that hydrolyzed the ester bond linearizing daptomycin (D'Costa et al., 2012).

Given that the predicted gramillin degradation products highlight the cleavage of an amide bond, we hypothesized that the proteolytic degradation of gramillin could be supported by the identification of 14 apoplast localized proteases identified in our barley leaf fluid proteomics dataset. We focused on the apoplastic space since previous work with Arabidopsis has linked gramillin-induced host responses to at least three plasma membrane localized signaling components RBOHD, BIK1 and ILK1 (Brauer et al., 2024). Comparisons between the proteomics and transcriptomics dataset revealed downregulation of HORVU.MOREX.r3.4HG0342480 which encodes one of the candidate serine endopeptidases (F2CTD9) in both barley genotypes at 4 hours following gramillin treatment.

The detection of this protease in the barley leaf fluid, together with its transcriptional response to gramillin, suggests that this as a strong candidate enzyme for downstream functional testing of gramillin degradation.

A previous study on wheat apoplast fluid was able to purify a subtilisin-like serine protease linked to increased proteolytic activity when challenged by a leaf rust fungus *Puccinia triticina* which suggests that this is a potential response mechanism to pathogen invasion in cereals (Fan et al., 2016). In addition, barley also uses other enzymatic mechanisms for detoxifying *F. graminearum* metabolites such as the UDP-glucosyltransferase HvUGT13248 which converts DON to the less toxic DON-3-glucoside (Bethke et al., 2023). Overall, gramillin degradation may represent an innate barley detoxification process that reduces the persistence or the effective concentration of cyclic gramillin in the apoplastic space. Future work should focus on *in-silico* analysis of the substrate specificity of candidate proteolytic enzymes and how they might interact with the gramillin's cyclic ring to produce the predicted degradation products. Purifying candidate proteases and experimentally validating the gramillin degradation activity *in-vitro* would also be a valuable next step. Comparative analysis of gramillin degradation in wheat, barley and maize extracts could also provide insight into the species-level differences in gramillin sensitivity. Finally, increasing the abundance of the validated gramillin-degrading enzymes could be a novel strategy to mimic gramillin insensitivity in sensitive plant species.

4.3 Gramillin insensitivity may be due to limited cellular disruption

Cyclic lipopeptides can alter plasma membrane organization causing ion leakage and inducing cellular stress responses. For example, surfactin transiently inserts into the plasma membrane through preferential interactions with glucosylceramides (Gilliard et al., 2026). The resulting membrane remodeling activates MCA 1/2 and MSL10 mechanosensitive ion channels, leading to ion fluxes, transient transcriptional reprogramming compared to MAMPs, calcium influx and RBOHD independent ROS production (Gilliard et al., 2026). Surfactin does not cause substantial electrolyte leakage or reduce cell viability at defense inducing concentrations (Gilliard et al., 2026). By contrast, gramillin acts as a cation-conducting ionophore that disrupts ion balance and causes electrolyte leakage and tissue necrosis (Brauer et al., 2024). This damage is accompanied by extensive transcriptional reprogramming, callose deposition, calcium influx and a transient RBOHD dependent ROS burst (Brauer et al., 2024). Previous work has established that gramillin sensitivity is independent of inducible stress signaling such as early ROS and calcium dependent signaling (Brauer et al., 2024). Consistent with this, we confirmed that Lowe's insensitivity cannot be explained by a general defect in inducible stress signaling. More importantly, the contrast between surfactin and gramillin suggests that ionophore sensitivity may depend on the nature of their interaction with the plasma membrane.

In this study, gramillin induced stress responses in both Lowe and gramillin-sensitive barley varieties suggesting that Lowe is responsive to this toxin. However, while transcriptional reprogramming was at a similar magnitude at 30 minutes in Lowe and Leo following gramillin exposure, after 4 hours Lowe had reversed more of the transcriptional

changes than Leo. In eukaryotic cells, plasma membrane damage must be rapidly repaired to ensure survival hence repair responses can be coordinated by signaling kinases and membrane trafficking (Idone et al. 2008, Andrews et al. 2014). Therefore, enrichment of vesicle transport and signaling-associated genes in gramillin-sensitive Leo may suggest the sustained activation of cellular repair and stress adaptation pathways following gramillin exposure at 4 hours. In contrast, the attenuation of Lowe suggests limited gramillin induced damage or a more rapid restoration of cellular homeostasis after the initial exposure.

Recovery from ionophore mediated membrane perturbation can involve active removal of the compound, restoration of ion gradients and repair of damaged membrane regions (Huang et al., 2017; Frederiksen et al., 2024). For example, the *NarAB* encoded ABC transporter reduces the susceptibility of *Enterococcus faecium* to narasin, salinomycin and maduramicin likely through active export of these ionophores and reducing their continued activity at the membrane (Naemi et al., 2020). In *Mycolicibacterium aurum*, nigericin resistance was associated with a mutation in the negative regulator of a putative RND-family efflux pump that results in constitutive activation, export and resistance to the ionophore's antimicrobial activity (Huang et al., 2017; Frederiksen et al., 2024). Another nigericin resistance mechanism in *Mycolicibacterium aurum* was associated with the sodium-proton antiporter NhaA which likely promotes recovery by restoring ion homeostasis (Huang et al., 2017; Frederiksen et al., 2024).

Active membrane remodeling can also promote recovery following plasma-membrane disruption as well. For example, in *Caenorhabditis elegans*, recovery from membrane damage caused by the *Bacillus thuringiensis* pore forming toxin Cry5B was

dependent on small GTPases that regulate of vesicle trafficking namely, RAB-5 and RAB-11. RAB-5 promoted endocytosis of the damaged membrane components while RAB-11 supported membrane recycling and repair (Los et al., 2011). The cells were able to restore membrane integrity within 24 hours post treatment, whereas suppression of *rab-5* or *rab-11.1* impaired membrane repair and increased toxin sensitivity (Los et al., 2011).

These mechanisms provide potential pathways through which Lowe could recover from an initial gramillin disturbance. In this study, one of the candidate gramillin-responsive genes found in the QTL encodes a glycosyltransferase-like gene that was more strongly induced by gramillin in Lowe which may reflect an early cell-wall remodeling response. Its rice homologue*, BC10* encodes a Golgi-localized type II membrane protein involved in cell-wall polysaccharide biosynthesis. Loss of *BC10* reduces cellulose abundance and weakens the mechanical strength in rice tissue (Zhou et al., 2009). Thus, stronger induction of the barley homologue in Lowe could suggest reinforcement of physical barriers to limit tissue collapse. Alternatively, induction of this glycosyltransferase-like gene may reflect a detoxification response similar to observed HvUGT13248 mediated glycosylation and inactivation of DON in barley (Bethke et al., 2023). Thus, differential expression of this glycosyltransferase-like candidate could influence gramillin sensitivity through either structural wall reinforcement or a detoxification mechanism. However, since Lowe exhibited both reduced ion leakage and attenuated transcriptional response, the current evidence more strongly supports reduced or less stable gramillin interaction with the plasma membrane rather than enhanced repair alone.

The activity of membrane-active cyclic lipopeptides is strongly influenced by target membrane properties including lipid packing, sterol composition, surface charge and sphingolipid composition (Balleza et al., 2019). For example, surfactin preferentially associates with glucosylceramides and depletion of complex sphingolipids in the Arabidopsis *loh1* mutant reduces surfactin-induced membrane remodeling, intracellular ROS accumulation and induced systemic resistance (Gilliard et al., 2026). Daptomycin is another CLP ionophore that relies on membrane charge to form pores since we see its mode of action as being reliant on calcium ions and presence of phosphatidylglycerol in the target membrane (Zhang et al. 2014). Syringomycin E presents an example where depending on the type of membrane sterol, its channel formation is impacted differently with cholesterol causing significant reduction in pore formation whereas ergosterol and stigmasterol have weaker effects (Feigin et al. 1997). Thus, differences in lipid composition, packing or membrane charge can substantially alter cyclic lipopeptide insertion, ion-conducting activity and impact sensitivity. In this study, a second candidate gramillin-responsive gene found in the QTL that encodes an elongation of fatty acids protein 3-like protein and was downregulated in Lowe but not Leo. ELO-like enzymes contribute to very-long-chain fatty acid biosynthesis which are important precursors for sphingolipid biosynthesis (Batsale et al. 2021). Differential ELO activity could impact membrane properties such as membrane thickness and lipid packing which may limit physical insertion of gramillin into the membrane (Balleza et al., 2019). Alternatively, it could also impact membrane signaling directly since it is involved in biosynthesis of sphingolipids. For example, disruption or lack of glycosyl inositol phosphoryl ceramide in the membrane will impact salt stress sensing in

plants while reduction in membrane sphingolipid glucosylceramides reduces surfactin sensitivity directly as observed in the *loh1* mutant (Xiao & Zhou, 2023; Jiang et al., 2019; Gilliard et al., 2026). These findings suggest that variation in ELO activity could influence gramillin sensitivity by altering both the physical properties of the plasma membrane and impacting sphingolipid-depending signaling processes activated following membrane perturbation.

Overall, our results support a model in which Lowe responds to gramillin but limits its sustained activity in the membrane. Differences in sphingolipid composition, lipid packing or other membrane properties could reduce gramillin insertion into the membrane resulting in a transient early stress response and explain the lack of ion leakage and tissue damage which is observed in sensitive barley. Future work should directly compare plasma membrane lipid composition and biophysical properties between Lowe and sensitive genotypes as well as determine whether the QTL candidate genes influence gramillin membrane interactions.

4.4 Gramillin sensitivity influences *F. graminearum* secondary metabolite gene expression during infection

Fungal secondary metabolism diverts resources away from primary growth and developmental process and hence is actively regulated (Shwab & Keller, 2007; Rokas et al., 2020). This regulation is especially important during infection, when metabolites such as DON and fusaoctaxins contribute to host colonization (Jansen et al., 2005; Armer et al., 2024; Jia et al., 2019). Previous studies have established fungal regulatory networks and influence environmental factors on the production of specific secondary metabolites *in-vitro*

(Gardiner et al., 2009; Ponts et al., 2007; Ponts et al., 2009). Furthermore, studies have also established importance of active host signals for secondary metabolite regulation (Harris et al., 2016; Boedi et al., 2016). Here, we present evidence of gramillin-induced membrane damage or host responses can influence *F. graminearum* secondary metabolite gene expression during infection.

Previous work has shown that gramillin production is required for full induction of fusaoctaxin biosynthetic genes during Arabidopsis seeding and barley head infection. They also showed that host genes *ILK1* and *RBOHD* were required for a full gramillin-induced ROS response which aligned with fungal virulence gene induction in sensitive plants (Brauer et al., 2024). Interestingly, in this study fusaoctaxin biosynthetic genes were not impacted by the gramillin production or host sensitivity to gramillin similarly. This may be due to the use of leaf disks in this study as opposed to barley heads highlighting tissue-specific responses to gramillin (Jia et al., 2019; Brauer et al., 2024; Harris et al., 2016). Nevertheless, the presence of gramillin and host sensitivity to gramillin were associated with increased expression of fungal virulence genes including trichothecene (*TRI3, TRI9*) and culmorin (*Clm1*) biosynthetic genes during barley leaf infection. A comparable interaction happens during *F. graminearum* infection of wheat, where the host stress response associated production of a polyamine, putrescine, acts as an environmental cue that activates a FgAreA-dependent regulatory pathway promoting fungal *TRI* gene expression and DON biosynthesis (Gardiner et al., 2010; Ma et al., 2021). Together, these findings support a model in which gramillin-induced membrane damage and host responses can act as environmental cues that influence fungal secondary metabolite production pathways.

One possibility is the influence of higher cell lysis caused by the presence of gramillin in the sensitive host as compared to Lowe barley. Previous work has shown that gramillin induces a range of phytotoxic effects in different barley cultivars measured through ion-leakage and lesion formation (Power, 2024). Given that Lowe barley exhibits strong insensitivity against gramillin it may limit the amount of electrolyte or nutrient leakage out of the cells as compared to the sensitive variety which may be contributing to the earlier or stronger induction of fungal virulence genes observed in the leaf-disk infection system. A candidate host signal connecting gramillin induced host responses with fungal gene expression is the generation ROS. Gramillin has previously been shown to induce a ROS burst through host signaling components (Brauer et al., 2024). Recent work has also established a link between RBOHD-mediated ROS production and fungal virulence gene expression in Arabidopsis (Brauer et al., 2024). Furthermore, oxidative stress through addition of hydrogen peroxide has been linked to trichothecene biosynthesis through redox-responsive transcription factor FgAP1 in *F. graminearum* previously (Ponts et al. 2007; Ponts et al. 2009; Montibus et al. 2013). Therefore, one possibility is that gramillin-sensitive host tissue may generate an oxidative environment that the fungus senses this as a cue to activate secondary metabolite production. We observed that gramillin downregulates glutathione metabolic pathways at 30 mins in Lowe suggesting regulation of the oxidative state in the plant. Glutathione is an important antioxidant pathway in plants that helps maintain ROS homeostasis hence, a downregulation of these pathways potentially indicates that gramillin induces a differential ROS response in Lowe as compared with gramillin-sensitive Leo (Noctor et al. 2012). However, this mechanism remains hypothetical in the present study as

we were unable to measure ROS levels directly during infection. Thus, while the data support a connection between gramillin sensitivity, host response state, and fungal secondary metabolism, further experiments manipulating host ROS during infection would be required to determine whether ROS is the causal signal driving these transcriptional changes in the fungus. Future work will test the effects of ROS suppression using SHAM or DPI and increased oxidative conditions using exogenous hydrogen peroxide treatment on the expression of genes associated with trichothecene, culmorin and fusaoctaxin biosynthesis.

Interestingly, the transcriptional pattern was not mirrored by our metabolite analysis. This may reflect biological differences in the link between our target gene expression and metabolite accumulation. For example, *TRI3* encodes a trichothecene acetyltransferase involved in intermediate modification during DON biosynthesis, whereas the role of *TRI9* in trichothecene biosynthesis remains unclear (Garvey et al., 2009; Huang et al., 2024). Therefore, changes in *TRI3* or *TRI9* expression may not directly reflect differences in trichothecene-associated biosynthetic product accumulation. Furthermore, transcript abundance can change rapidly in response to the environment, whereas metabolite levels reflect the combined outcome of many genes working together to synthesize, transport and accumulate a metabolite over time (Gibon et al., 2006; Fernie and Stitt, 2012). Hence, the elevated expression of fungal secondary metabolite biosynthetic genes at 3 dpi indicates a snapshot of an active transcriptional state within the fungus that may not be reflected at the metabolite level yet. Future work should include a time-course analysis may provide more clarity on the timing, duration of gene induction and metabolite accumulation in this system. Direct fungal biomass quantification using fungal DNA-based qPCR relative to plant DNA

would be also an improvement instead of relying on fungal gene expression as a normalization measure to discern if observed trends in metabolite accumulate are due to an impact on fungal secondary metabolism or simply differences in fungal abundance (Kumar et al., 2015).

Overall, a major implication of the observed impact of gramillin sensitivity on fungal gene expression is that it suggests gramillin induced host responses are relevant during infection. This is consistent with previous work where gramillin was shown to promote fungal virulence by inducing RBOHD-dependent ROS responses (Brauer et al., 2024). Much of the previous work on CLP ionophore-induced plant responses has focused on their ability to prime host defense responses against subsequent pathogen attack (Ongena et al. 2007; Ding et al., 2025). For example, *Bacillus*-derived surfactin mediates the activation of plant defense responses against *Botrytis cinrea* infection through membrane lipid signaling components (Gilliard et al., 2026). Similarly, *Pseudomonas* derived medpeptin activates a localized cell death response using cell-wall associated signaling kinases to confer resistance against pathogen infection (Gu et al. 2023). These examples highlight how host sensitivity to membrane-active microbial metabolites can be beneficial for the plant from a disease resistance perspective. However, we also observe that pathogen-derived metabolites can promote disease by manipulating host physiology in ways that favor infection. For example, *Pseudomonas syringae* produces coronatine which mimics hormonal signaling pathways in the plant, triggers stomatal opening and promotes pathogen penetration (Zheng et al., 2012). Similarly, *Phomopsis amygdali* produces fusicoccin that activates plasma membrane proton pumps to cause irreversible stomatal opening, water

loss and wilting (Marra et al., 2021). Hence, host sensitivity to microbial metabolites is not strictly protective and can be exploited by pathogens to promote disease and gramillin is an example of this phenomenon.

5. Conclusions

Overall, this study proposes limited gramillin-induced membrane disruption in Lowe as the basis for insensitivity rather than complete avoidance or enhanced degradation. Furthermore, this study identifies host gramillin sensitivity as a potential factor shaping *F. graminearum* secondary metabolite gene expression during barley leaf infection. Genetic tracking of gramillin sensitivity using KASP markers provide an efficient method to genotype diverse barley varieties for this trait. Future work will establish whether gramillin insensitivity is consistently associated with reduced mycotoxin accumulation during F. *graminearum* infection in barley leaf and head tissue. Given the substantial economic impact of FHB, this work could provide breeders with a new avenue for improving FHB resistance and ultimately help protect the quality, value, and sustainability of barley production for farmers and maltsters globally.

6. Figures

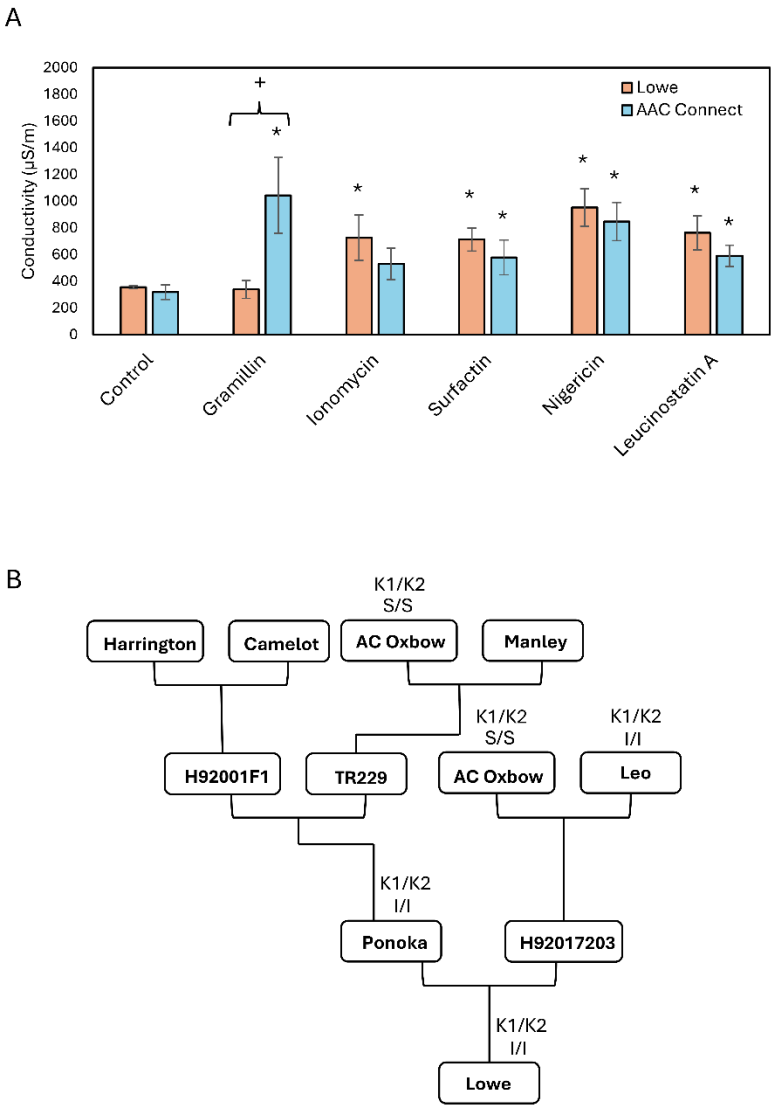

Figure 3: Lowe's insensitivity is specific to the gramillin ionophore

A) Conductivity of Lowe and Connect barley leaf disks 24 hours after treatment with ionomycin (50 µM), surfactin (500 µM), nigericin (50 µM), leucinostatin A (20 µM) and gramillin (20 µM) (n=4). Statistical significance was determined using a one-way ANOVA with

post-hoc Tukey's HSD ($p < 0.05$). An asterisk denotes treatment differed significantly from the 5% DMSO control, and a cross denotes significant differences between genotypes. This experiment was repeated three times with similar results.

B) Lowe barley's parental lineage annotated with the observed KASP signal. This experiment was repeated three times with similar results. Figure legend; S=gramillin sensitivity allele, I=gramillin insensitivity allele. K1 = KASP1 marker and K2 = KASP2 marker

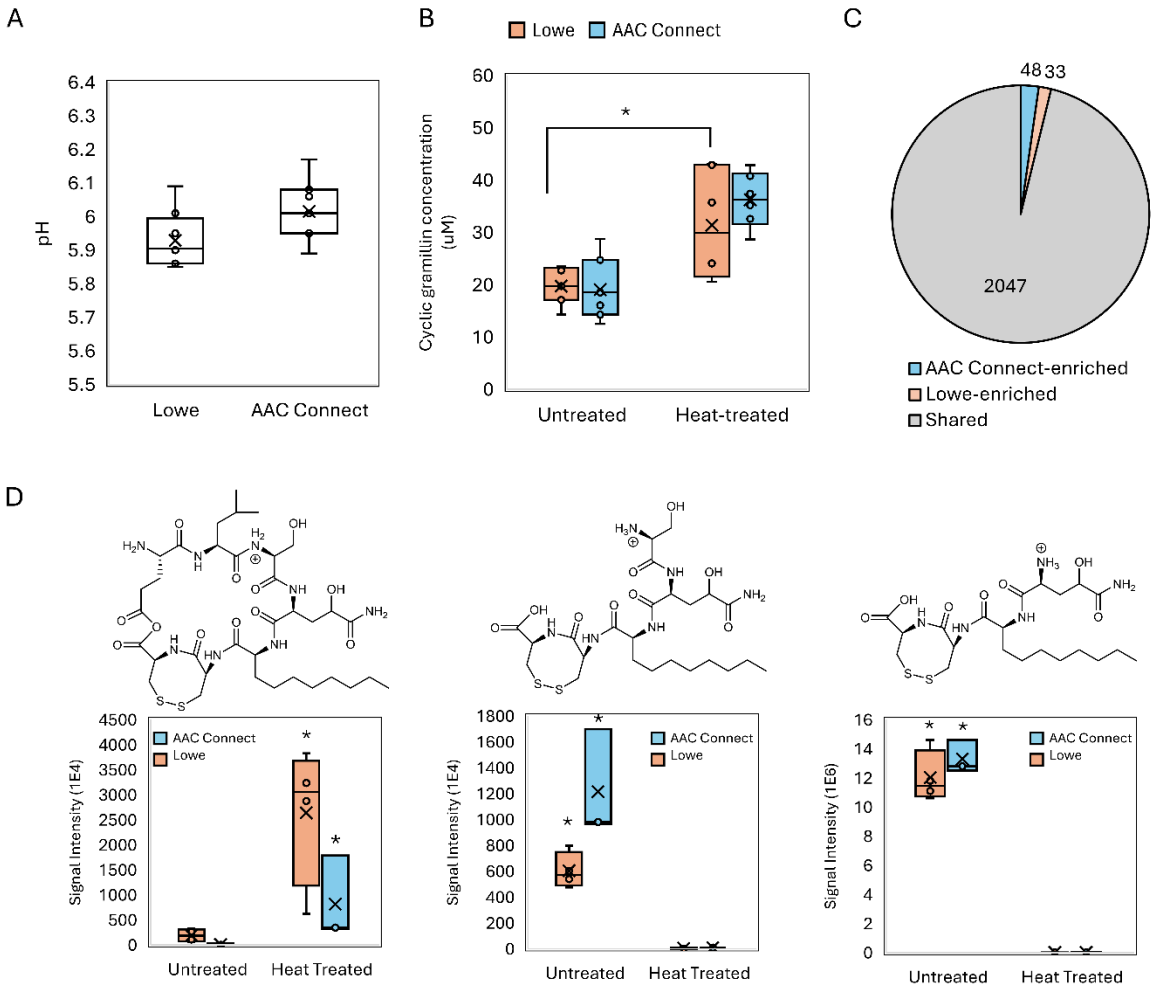

Figure 4: Gramillin degradation is similar between barley genotypes.

A) The average pH measurement of barley leaf fluid extracted from 2-week-old AAC Connect and Lowe barley leaves (n=7-8). No significant differences were observed between genotypes.

B) Apoplastic fluid from 2-week-old Connect and Lowe barley leaves was incubated with 40 µM gramillin for 30 minutes at room temperature. No significant differences were observed between genotypes. Asterisk denotes significant differences from the respective untreated control ($p < 0.05$, two-tailed Student's t-test). Data presented was pooled from two independent trials (n=3).

C) Pie chart summarizing the proteomic profiling of APF extracts from both genotypes (n=3). Relative genotypic abundances were determined based on average delta log2 intensity value > 2.

D) Metabolomic profiling of cyclic gramillin and gramillin degradation products identified from the same samples used for the apoplastic fluid gramillin degradation assay. Data presented was pooled from two independent trials (n=2-3). Asterisk denotes significant differences from the respective untreated control ($p < 0.05$, two-tailed Student's t-test). Data presented was pooled from two independent trials (n=3). *Data analysis by Dr. Tom Witte.*

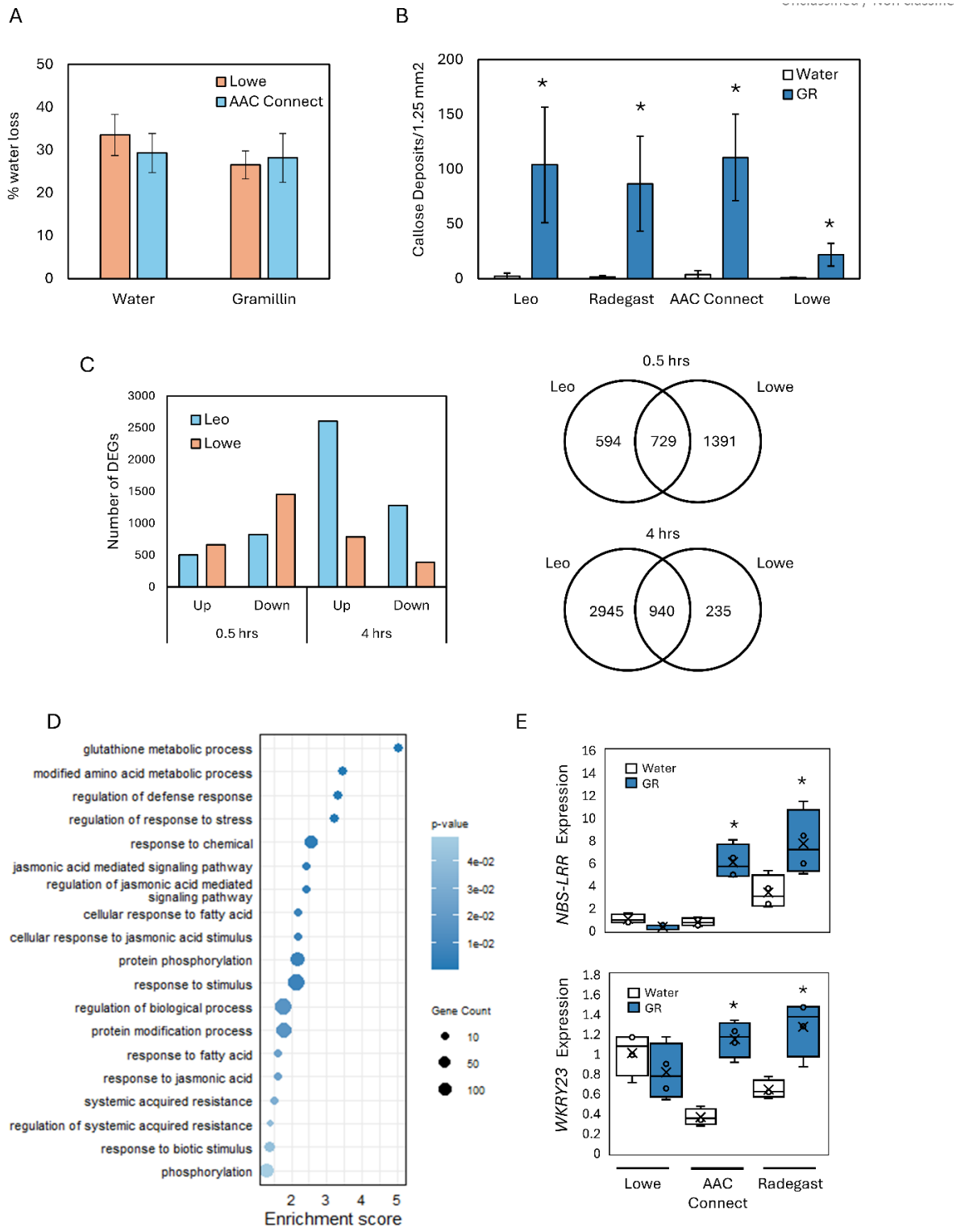

Figure 5: Gramillin-induces shorter and smaller stress responses in Lowe to gramillin-sensitive barley.

A) The average water loss of injected barley leaf sections (5 cm) is expressed as a percentage relative to the starting leaf weight 2-hours after syringe infiltration with water or 10 µM gramillin (n=5). The data presented is from a single trial and three replicate trials were conducted with similar trends.

B) Gramillin induced callose deposition in barley genotypes 24 hours after treatment with 5 µM gramillin. The number of cells producing callose was visualized by microscopy after aniline blue staining (n=10). The experiment was repeated three times with similar results. Statistical significance was determined using a one-way ANOVA with post-hoc Tukey's HSD ($p < 0.05$). An asterisk denotes treatment differed significantly from its own water control, and a cross denotes significant differences between genotypes. *Data generated by Whynn Bosnich*.

C) Transcriptional profiling of Lowe and Leo barley leaves following water or 5 µM gramillin treatment at 0.5 and 4 hours (n=4). Differentially expressed genes (DEGs) were selected by comparing gramillin induced expression to water and a threshold of log2 fold change>1. Venn diagram highlighting gramillin induced DEG overlap between genotypes at 0.5 and 4 hours.

D) Bubble plot representing GO enrichment analysis conducted on 1,391 uniquely downregulated genes in Lowe barley at 30 minutes after 5 µM gramillin treatment. *P* values were adjusted for multiple comparisons using the g:SCS algorithm from g:Profiler. The top 20 significantly enriched GO terms from the Biological Processes (BP) classification are presented here.

E) Gramillin induced gene expression at 4 hours after water or 5 µM gramillin treatment of Lowe, Radegast and AAC Connect barley seedling leaves using quantitative PCR (n=4). The housekeeping genes *Actin* and *Cyclophilin* were used for normalization. The experiment was repeated three times with similar results. In both panels * indicates that the treatment differs significantly from the water control at the $p<0.05$ level using a one-way ANOVA with post-hoc Tukey's HSD test.

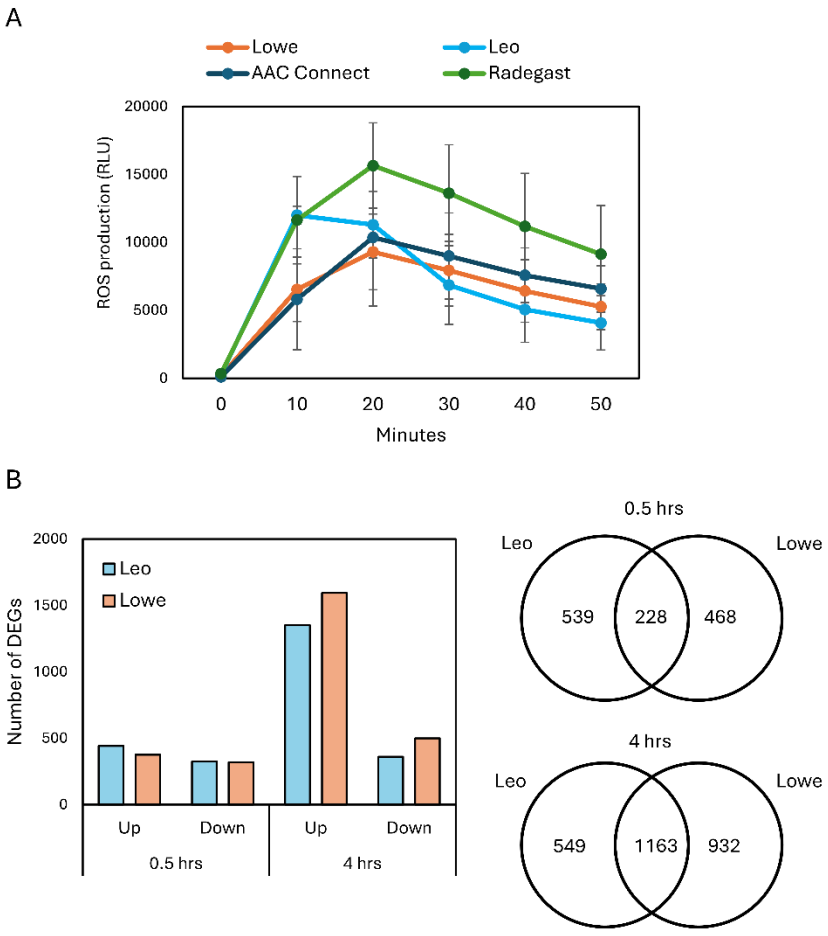

Figure 6: Lowe barley has intact inducible stress responses.

A) Gramillin-sensitive and insensitive genotypes of barley produce an intact flg22-induced ROS burst (n=6). This experiment was repeated three times with similar results. *Data generated by Whynn Bosnich*.

B) Transcriptional profiling of Lowe and Leo barley leaves following water or 1 μM flg22 treatment at 0.5 and 4 hours (n=4). Differentially expressed genes (DEGs) were selected by comparing flg22-induced gene expression to water and a threshold of log2fold change>1 C) Venn diagram highlighting flg22-induced DEG overlap between genotypes at 0.5 and 4 hours.

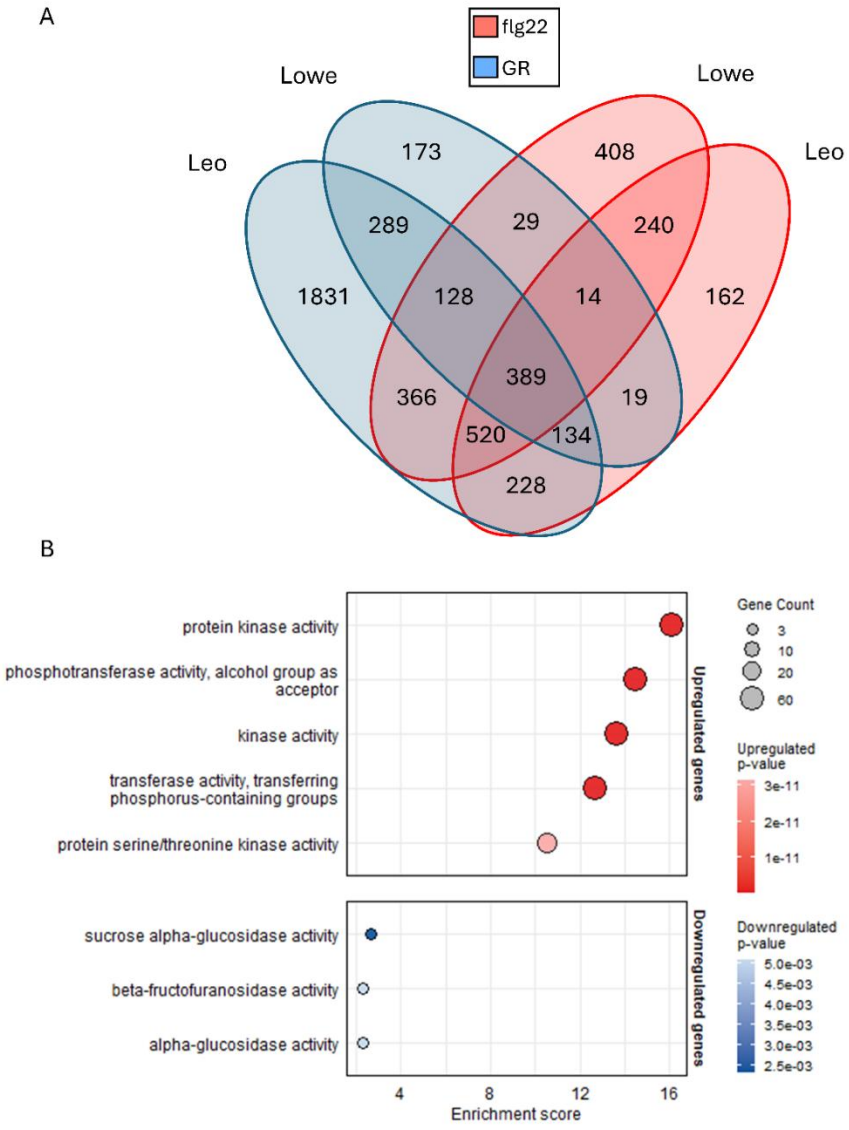

Figure 7: Overlap in transcriptional reprogramming induced by gramillin and flg22 in barley genotypes

A) Venn diagrams highlighting overlap of differentially expressed genes (DEGs) in response to gramillin and flg22 treatments in Lowe and Leo barley at 4 hours.

B) GO enrichment analysis of 265 shared upregulated (top) and 123 shared downregulated (bottom) DEGs shared between Lowe and Leo genotypes and in both treatments at 4 hours.

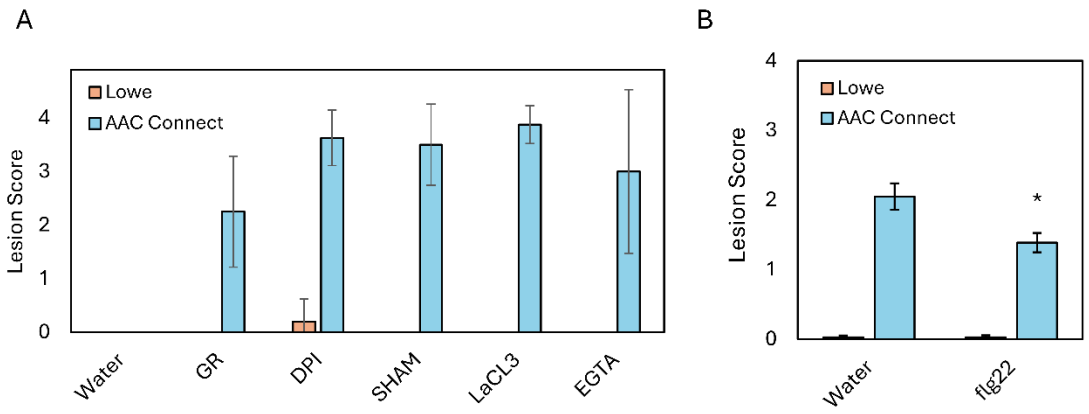

Figure 8: Gramillin induced lesion assays in two-week-old Lowe and Connect barley.

Lesion severity within the infiltrated region was evaluated 24 hours after treatment by visual assessment was done as follows; 0 = no necrosis, 1 = 1-25%, 2 = 26-50%, 3 = 51-75% and 4 = 76-100%. Statistical significance ($p<0.05$) from the control was determined by a one-tailed Student's t-test and is indicated by an asterisk.

A) Co-infiltration with chemical inhibitors shows no induction of lesions in Lowe, while Connect responses remain unchanged relative to their own water control. Data represents average ± SD (n = 7-11). Results from one of two independent trials are shown, both of which yielded similar results.

B) Quantification of lesion severity in Lowe and AAC Connect barley leaves 24 hours after infiltration with 10 µM gramillin, following a 24-hour pre-treatment with either water or 1 µM flg22. Data represents mean ± SEM from pooled results of three independent experiments (n = 36–44 biological replicates per treatment).

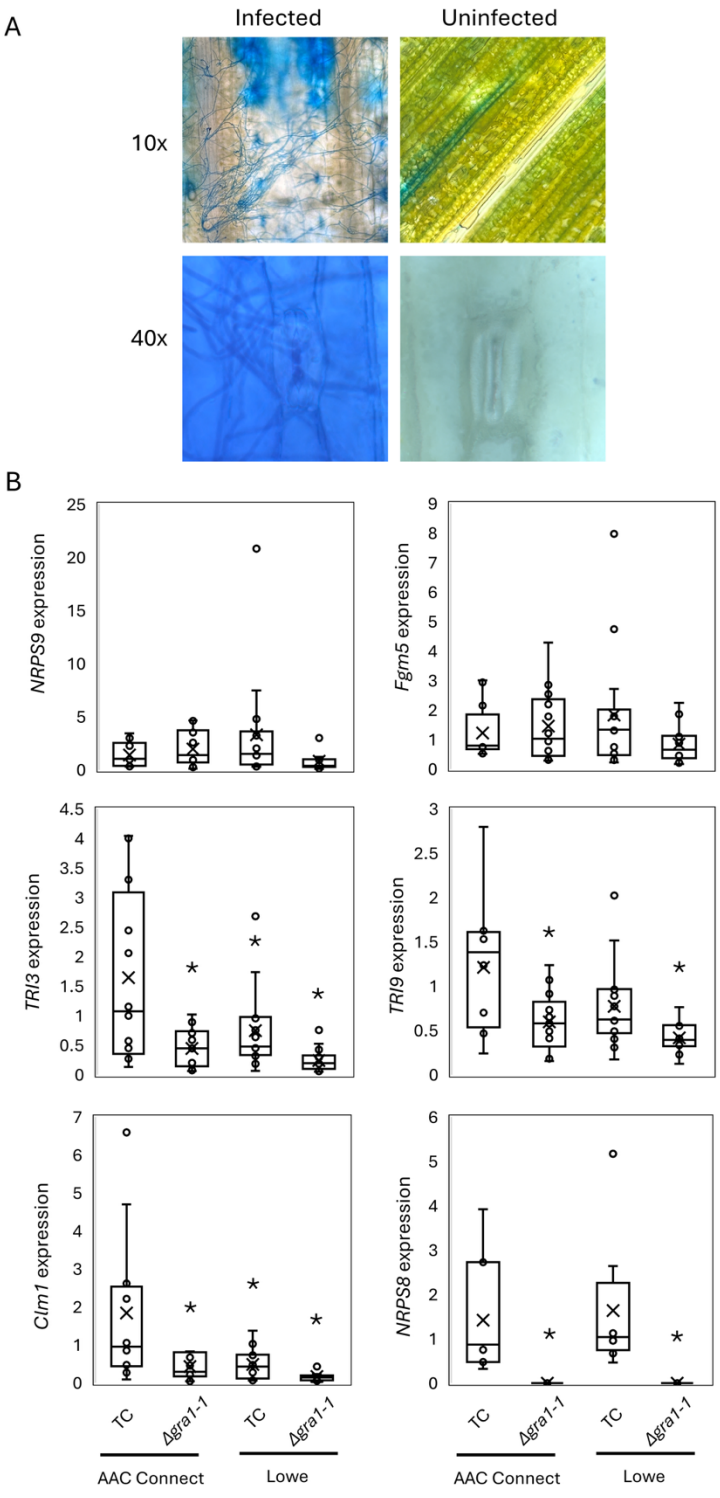

Figure 9: Host gramillin sensitivity influences expression of specific fungal genes

A) Representative images of mycelial penetration in infected barley leaf disks 3 days post-inoculation (dpi).

B) Relative gene expression analysis of fungal genes 3 dpi of AAC Connect or Lowe barley leaf disks (4mm) by *Δgra1-1* mutant or transformation control (TC) fungal strain using qPCR (n=4-5). The fungal housekeeping genes *GAPDH* and *β-tubulin* were used for normalization. Statistical significance ($p<0.05$) was determined by one way ANOVA and post hoc Tukey's test and the asterisks (*) denotes significant differences from the TC-AAC Connect treatment condition. Data represents pooled results of three independent experiments.

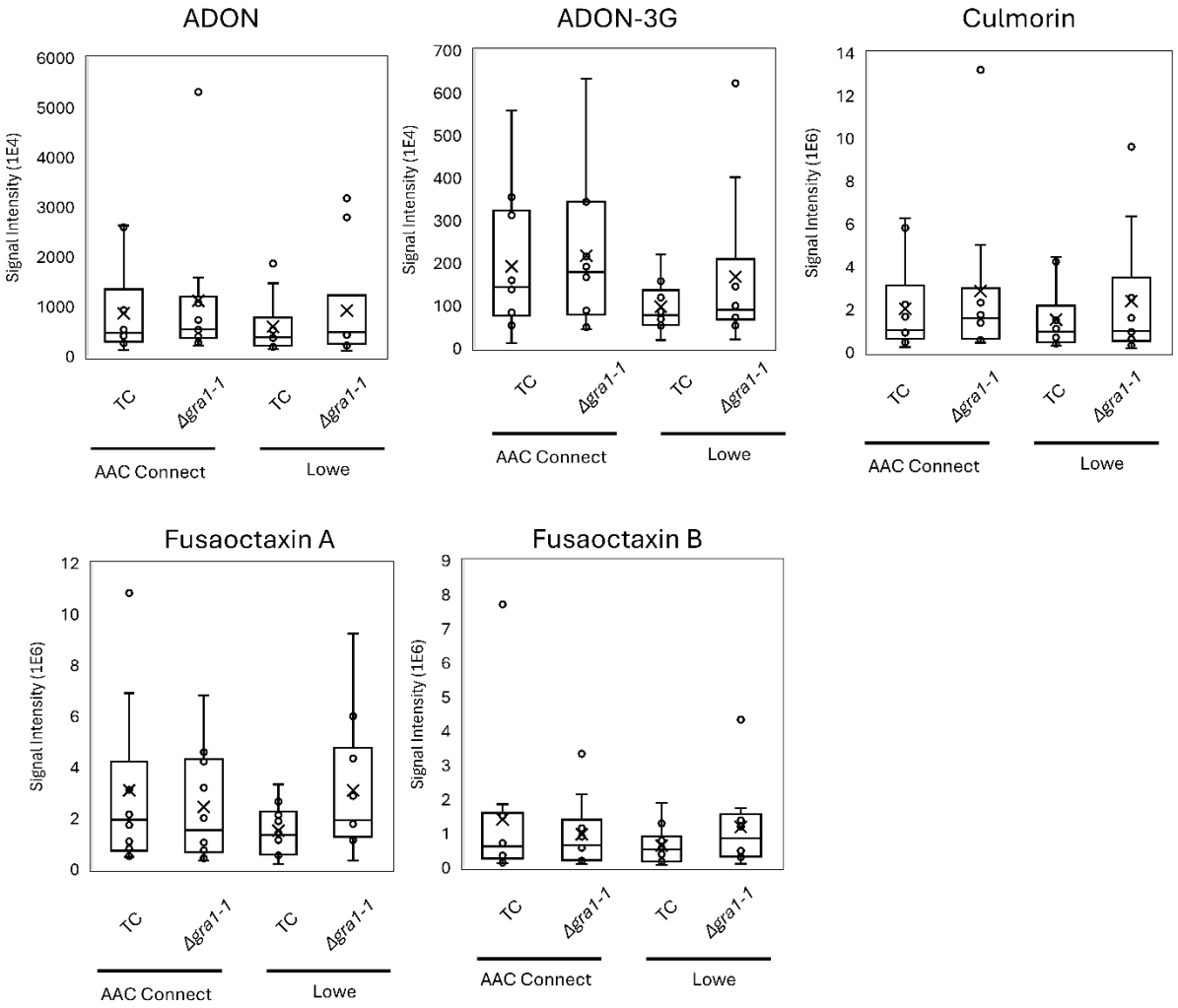

Figure 10: Metabolomic profiling of infected barley leaf disks

Relative signal intensity of ADON, ADON-3G, Culmorin, Fusaoctaxin A and Fusaoctaxin B during infection of AAC Connect or Lowe barley leaf disks (4mm) by *Δgra1-1* mutant or transformation control (TC) fungal strain using metabolomics approach (n=7-10). Data represents pooled results of two independent experiments.

7. Tables

Table 1: KASP primers used to track SNPs associated with gramillin sensitivity or insensitivity in Lowe-related barley genotypes.

Primer Set	SNP	Location on 5H chromosome (bp)	Allele	Primer Sequence
KASP 1	S5H_2645485	2,645,485	Sensitive	GAAGGTGACCAAGTTCATGCTagatccagatccaggttatccttC
			Insensitive	GAAGGTCGGAGTCAACGGATTagatccagatccaggttatccttT
			Both	cgctgaaatttcctccgtgg
KASP 2	S5H_2468415	2,468,415	Insensitive	GAAGGTGACCAAGTTCATGCTcatgcgccgtcttcttcatT
			Sensitive	GAAGGTCGGAGTCAACGGATTcatgcgccgtcttcttcatC
			Both	gaagcttgtgaaggggctgc

Table 2: Validation of KASP-based genotyping for gramillin sensitivity within Lowe-derived populations. Progeny from the Lowe x AAC Connect population is indicated in grey while progeny from Lowe x Radegast population are in white in the genotype column. The sequencing-based identification of the sensitive (S) or insensitive (I) allele is indicated in SNP1 and SNP2 column. The KASP result for each genotype was determined experimentally on 2-3 different plants for each genotype. The dash indicates information that was not available.

Genotype	K1	SNP 1	K2	SNP 2
Lowe	I	I	I	I
AAC Connect	S	S	I	-
Radegast	S	S	S	S
T18122013	I	I	I	-
T18122043	I	I	I	-
T18122044	I	I	I	-
T18122056	I	I	I	-
T18122091	I	I	I	-
T18122093	I	I	I	-
T18122008	S	S	I	-
T18122015	S	S	I	-
T18122034	S	S	I	-
T18122084	S	S	I	-
T19142015	S	S	S	S
T19142043	S	I	S	I
T19142080	I	I	I	I
T19142082	S	S	S	S
T19142083	I	I	I	I
T19142092	I	I	I	I
T19142094	S	S	S	S
T19142033	S	S	S	S
T19142048	S	S	S	S
T19142084	S	S	I	S
Ponoka	I	-	I	-
Leo	I	-	I	-
AC Oxbow	S	-	S	-

Table 3: List of primers used for quantitative RT-PCR. The species of organism which the primer is targeting is indicated as *Hv* for *Hordeum vulgare* or *Fg* for *Fusarium graminearum*.

Gene	Species	Forward Primer	Reverse Primer	Gene ID
WRKY23	*Hv*	CATAGCTAGCTCCCCGGTTG	TGACATTCCTGAATTGCACACTG	*HORVU.MOREX.r3.1HG0092420*
NBS-LRR	*Hv*	ACTACAGGCAGAAGAACGCC	AGGAACAGCTTGAGACGACC	*HORVU.MOREX.r3.1HG0081690*
Actin	*Hv*	GATCAAGGTCGTCGCTCCAC	TGGAAAGTGCTGAGTGAGGC	*HORVU.MOREX.r3.1HG0003140*
Cyclophilin	*Hv*	CTCTGTTTCACAGGGAGGTCT	CGCACGATGCACAACAAAGA	*HORVU.MOREX.r3.7HG0689490*
NRPS9	*Fg*	TTTGGGCCATGTCACTCCTC	CCGCCACGGCTAATTTGATG	*FGSG_10990*
TRI5	*Fg*	GGCCCAAGGACCTGTTTGAT	CAACGGCTGACGTGATTTCA	*FGSG_03537*
GAPDH	*Fg*	TGACTTGACTGTTCGCCTCGA	ATGGAGGAGTTGGTGTTGCC	*FGSG_16627*
β-tubulin	*Fg*	CATGCAAATGTCGTAGAGGG	GTTGATCTCCAAGATCCGTG	*FGSG_09530*
NRPS8	*Fg*	CTCGCATAGCATACCTACATCAA	CGAGATGAGCGAGAAGAAGAAG	*FGSG_11659*
NRPS9	*Fg*	TTTGGGCCATGTCACTCCTC	CCGCCACGGCTAATTTGATG	*FGSG_10990*
Fgm5	*Fg*	CGACAATTCCTTTGGCCCGA	ACGAGTGAGTGCTAGCAGGA	*FGSG_10995*
TRI5	*Fg*	GGCCCAAGGACCTGTTTGAT	CAACGGCTGACGTGATTTCA	*FGSG_03537*
TRI3	*Fg*	CACCCTTGGTACCAGCACTT	CTCTTCCAGTCCAACAATTGCC	*FGSG_03534*
TRI9	*Fg*	GCGGGGATCTTCACAAGGAA	CGAATCAGTGCTGTGTCCCT	*FGSG_03539*
Clm1	*Fg*	TTGTGGCTCGCAAGGGTATT	TCCAGGTTGGGGAATTGTCG	*FGSG_10397*

8. Supplementary Data

Supplementary Data 1: Proteomic profiling of plant apoplastic fluid from Lowe and AAC Connect barley. Three replicate samples per genotype were used dataset generation and curation.

A: Differentially abundant proteins.

B: List of candidate apoplast-localized proteases and their expression following GR or flg22 exposure.

Supplementary Data 2: Transcriptional profiling of Lowe and Leo barley leaves in response to 5 μM gramillin or 1 μM flg22 relative to a water control. Three or four replicate samples were used per treatment.

A: Differentially expressed genes in Leo barley leaves following syringe injection with 5 μM purified gramillin treatment for 0.5 hours relative to water.

B: Differentially expressed genes in Lowe barley leaves following syringe injection with 5 μM purified gramillin treatment for 0.5 hours relative to water.

C: Differentially expressed genes in Leo barley leaves following syringe injection with 5 μM purified gramillin treatment for 4 hours relative to water.

D: Differentially expressed genes in Lowe barley leaves following syringe injection with 5 μM purified gramillin treatment for 4 hours relative to water.

E: Differentially expressed genes in Leo barley leaves following syringe injection with 1 μM flg22 treatment for 0.5 hours relative to water.

F: Differentially expressed genes in Lowe barley leaves following syringe injection with 1 μM flg22 treatment for 0.5 hours relative to water.

G: Differentially expressed genes in Leo barley leaves following syringe injection with 1 μM flg22 treatment for 4 hours relative to water.

H: Differentially expressed genes in Lowe barley leaves following syringe injection with 1 μM flg22 treatment for 4 hours relative to water.

I: Venn diagram analysis of differentially expressed genes overlaps between treatments, genotypes and timepoints.

J: Differentially expressed genes in the 5H QTL region associated with gramillin sensitivity.

Supplementary Data 3: Enrichment analysis of differentially expressed genes in Lowe and Leo genotypes in response to 5 μM gramillin or 1 μM flg22 relative to a water control.

A: Gene ontology enrichment results on shared DEGs between Lowe and Leo genotype induced 0.5 hours after 5 μM gramillin treatment.

B: Gene ontology enrichment results on shared DEGs between Lowe and Leo genotype induced 4 hours after 5 μM gramillin treatment.

C: Gene ontology enrichment results on unique DEGs in Lowe genotype induced 0.5 hours after 5 μM gramillin treatment.

D: Gene ontology enrichment results on unique DEGs in Leo genotype induced 4 hours after 5 μM gramillin treatment.

E: Gene ontology enrichment results on unique DEGs in Lowe genotype induced 4 hours after 5 μM gramillin treatment.

F: Gene ontology enrichment results on shared DEGs between Lowe and Leo genotype induced 4 hours after 1 μM flg22 treatment.

G: Gene ontology enrichment results on shared upregulated DEGs between Lowe and Leo genotype induced 4 hours after both treatments 1 μM flg22 and 5 μM gramillin treatment.

H: Gene ontology enrichment results on shared downregulated DEGs between Lowe and Leo genotype induced 4 hours after both treatments 1 μM flg22 and 5 μM gramillin treatment.

I: Gene ontology enrichment results on unique DEGs in Leo genotype induced 0.5 hours after 5 μM gramillin treatment.

9. References

Alatossava, T., Vaara, M., & Baschong, W. (1984). Polymyxin B nonapeptide sensitizes *Escherichia coli* to valinomycin and A23187 ionophores. *FEMS Microbiology Letters*, *22*(3), 249‑251. https://doi.org/10.1111/j.1574-6968.1984.tb00736.x

Alisaac, E., & Mahlein, A.-K. (2023). Fusarium head blight on wheat: Biology, modern detection and diagnosis and integrated disease management. *Toxins*, *15*(3), 192. https://doi.org/10.3390/toxins15030192

Andrews, N. W., Almeida, P. E., & Corrotte, M. (2014). Damage control: Cellular mechanisms of plasma membrane repair. *Trends in Cell Biology*, *24*(12), 734–742. https://doi.org/10.1016/j.tcb.2014.07.008

Angélica Gutiérrez-Sánchez, Plasencia, J., Monribot-Villanueva, J. L., Benjamín Rodríguez-Haas, Eliel Ruíz-May, Guerrero-Analco, J. A., & Sánchez-Rangel, D. (2023). Virulence factors of the genus Fusarium with targets in plants [Review of *Virulence factors of the genus Fusarium with targets in plants*]. *Microbiological Research*, *277*, 127506–127506. https://doi.org/10.1016/j.micres.2023.127506

Bahadoor, A., Brauer, E. K., Bosnich, W., Schneiderman, D., Johnston, A., Aubin, Y., Blackwell, B., Melanson, J. E., & Harris, L. J. (2018). Gramillin A and B: Cyclic Lipopeptides Identified as the Nonribosomal Biosynthetic Products of *Fusarium graminearum*. *Journal of the American Chemical Society*, *140*(48), 16783–16791. https://doi.org/10.1021/jacs.8b10017

Balleza, D., Alessandrini, A., & Beltrán García, M. J. (2019). Role of Lipid Composition, Physicochemical Interactions, and Membrane Mechanics in the Molecular Actions of

Microbial Cyclic Lipopeptides. *The Journal of Membrane Biology*, *252*(2–3), 131–157. https://doi.org/10.1007/s00232-019-00067-4

Batsale, M., Bahammou, D., Fouillen, L., Mongrand, S., Joubès, J., & Domergue, F. (2021). Biosynthesis and Functions of Very-Long-Chain Fatty Acids in the Responses of Plants to Abiotic and Biotic Stresses. *Cells*, *10*(6), 1284. https://doi.org/10.3390/cells10061284

Beattie, A., Badea , A., & Tucker, J. (2023, March 3). *FHB screening of CDC barley breeding selections, 2016-2020 - SaskBarley*. SaskBarley. https://saskbarley.com/projects/fhb-screening-of-cdc-barley-breeding-selections-2016-2020/

Benyamin, M. S., Perisin, M. P., Hellman, C. A., Schwalm, N. D, Jahnke, J. P., & Sund, C. J. (2023). Modeling control and transduction of electrochemical gradients in acid-stressed bacteria. *iScience*, *26*(7), 107140. https://doi.org/10.1016/j.isci.2023.107140

Beratto, M. E. (1990). Leo-INIA/CCU, a new malting barley cultivar [Review of *Leo-INIA/CCU, a new malting barley cultivar*]. *Agric. Técnica (Santiago)*, *50*, 89–90.

Bjornson, M., Dandekar, A., & Dehesh, K. (2015). Determinants of timing and amplitude in the plant general stress response. *Journal of Integrative Plant Biology*, *58*(2), 119–126. https://doi.org/10.1111/jipb.12373

Bjornson, M., Pimprikar, P., Nürnberger, T., & Zipfel, C. (2021). The transcriptional landscape of Arabidopsis thaliana pattern-triggered immunity [Review of *The transcriptional landscape of Arabidopsis thaliana pattern-triggered immunity*]. *Nature Plants*, *7*(5). https://doi.org/10.1038/s41477-021-00874-5

Boedi, S., Berger, H., Sieber, C., Münsterkötter, M., Maloku, I., Warth, B., Sulyok, M., Lemmens, M., Schuhmacher, R., Güldener, U., & Strauss, J. (2016). Comparison of Fusarium graminearum Transcriptomes on Living or Dead Wheat Differentiates

Substrate-Responsive and Defense-Responsive Genes [Review of *Comparison of Fusarium graminearum Transcriptomes on Living or Dead Wheat Differentiates Substrate-Responsive and Defense-Responsive Genes*]. *Frontiers in Microbiology*, *7*(1113), 1113. https://doi.org/10.3389/fmicb.2016.01113

Boller, T., & Felix, G. (2009). A Renaissance of Elicitors: Perception of Microbe-Associated Molecular Patterns and Danger Signals by Pattern-Recognition Receptors. *Annual Review of Plant Biology*, *60*(1), 379–406. https://doi.org/10.1146/annurev.arplant.57.032905.105346

Bosnich, W., Hoffmann, N., Lakshmanan, S., & Brauer, E. K. (2025). Evaluating Leaf Responses to Microbial Secondary Metabolites Using A High-Throughput Format. *Journal of Visualized Experiments : JoVE*, *226*, 10.3791/69026. https://doi.org/10.3791/69026

Brauer, E. K., Bosnich, W., Holy, K., Thapa, I., Krishnan, S., Moatter Syed, Bredow, M., Sproule, A., Power, M., Johnston, A., Cloutier, M., Haribabu, N., Izhar U.H. Khan, Diallo, J.-S., Monaghan, J., Chabot, D., Overy, D. P., Subramaniam, R., Piñeros, M., … Harris, L. J. (2024). A cyclic lipopeptide from Fusarium graminearum targets plant membranes to promote virulence. *Cell Reports*, *43*(7), 114384. https://doi.org/10.1016/j.celrep.2024.114384

Brauer, E. K., Bosnich, W., Power, M., Luckert, D., Khanal, S., Liang, N., James, R., Syed, M., Charette, M., Wolfe, D., Pattang, A., Morrison, H., Poncos, S., Laniel, M., Tucker, J., Khanal, R., Parent, J.-S., & Samanfar, B. (2025). Transcriptional Profiling and Genetic Mapping of Barley Responses to Bacterial Flagellin. *Molecular Plant-Microbe Interactions®*, *38*(2). https://doi.org/10.1094/mpmi-12-24-0159-fi

Burton, R. A., Shirley, N. J., King, B. J., Harvey, A. J., & Fincher, G. B. (2004). The *CesA* Gene Family of Barley. Quantitative Analysis of Transcripts Reveals Two Groups of Co-Expressed Genes. *Plant Physiology*, *134*(1), 224–236. https://doi.org/10.1104/pp.103.032904

Buttar, Z. A., Cheng, M., Wei, P., Zhang, Z., Chunlei Lv, Zhu, C., Ali, N. F., Kang, G., Wang, D., & Zhang, K. (2024). Update on the Basic Understanding of Fusarium graminearum Virulence Factors in Common Wheat Research. *Plants*, *13*(8), 1159–1159. https://doi.org/10.3390/plants13081159

Callaway, T. R., & Russell, J. B. (1999). Selection of a Highly Monensin-Resistant *Prevotella bryantii* Subpopulation with Altered Outer Membrane Characteristics. *Applied and Environmental Microbiology*, *65*(11), 4753–4759. https://doi.org/10.1128/aem.65.11.4753-4759.1999

Chen, A., Islam, T., & Ma, Z. (2022). An integrated pest management program for managing Fusarium head blight disease in cereals. *Journal of Integrative Agriculture*, *21*(12), 3434–3444. https://doi.org/10.1016/j.jia.2022.08.053

Chen, K.-E., Karinshak, M., & Vierstra, R. D. (2025). Streamline Protocol for *Arabidopsis* Apoplastic Fluid Isolation Enables a Detailed Proteomic View of the Plant Extracellular Space. *Plant Direct*, *9*(7), e70087. https://doi.org/10.1002/pld3.70087

Couto, D., & Zipfel, C. (2016). Regulation of pattern recognition receptor signalling in plants. *Nature Reviews. Immunology*, *16*(9), 537–552. https://doi.org/10.1038/nri.2016.77

Crisp, P. A., Ganguly, D., Eichten, S. R., Borevitz, J. O., & Pogson, B. J. (2016). Reconsidering plant memory: Intersections between stress recovery, RNA turnover, and epigenetics. *Science Advances*, *2*(2), e1501340. https://doi.org/10.1126/sciadv.1501340

Crouzet, J., Arguelles-Arias, A., Dhondt-Cordelier, S., Cordelier, S., Pršić, J., Hoff, G., Mazeyrat-Gourbeyre, F., Baillieul, F., Clément, C., Ongena, M., & Dorey, S. (2020). Biosurfactants in Plant Protection Against Diseases: Rhamnolipids and Lipopeptides Case Study. *Frontiers in Bioengineering and Biotechnology*, *8*. https://doi.org/10.3389/fbioe.2020.01014

D'Costa, V. M., Mukhtar, T. A., Patel, T., Koteva, K., Waglechner, N., Hughes, D. W., Wright, G. D., & De Pascale, G. (2011). Inactivation of the lipopeptide antibiotic daptomycin by Hydrolytic mechanisms. *Antimicrobial Agents and Chemotherapy*, *56*(2), 757–764. https://doi.org/10.1128/aac.05441-11

Debois, D., Fernandez, O., Franzil, L., Jourdan, E., de Brogniez, A., Willems, L., Clément, C., Dorey, S., De Pauw, E., & Ongena, M. (2015). Plant polysaccharides initiate underground crosstalk with bacilli by inducing synthesis of the immunogenic lipopeptide surfactin. *Environmental Microbiology Reports*, *7*(3), 570–582. https://doi.org/10.1111/1758-2229.12286

DeFalco, T. A., & Zipfel, C. (2021). Molecular mechanisms of early plant pattern-triggered immune signaling. *Molecular Cell*, *81*(17), 3449–3467. https://doi.org/10.1016/j.molcel.2021.07.029

Ding, N., Dong, H., & Ongena, M. (2025). Bacterial Cyclic Lipopeptides as Triggers of Plant Immunity and Systemic Resistance Against Pathogens. *Plants*, *14*(17), 2644–2644. https://doi.org/10.3390/plants14172644

Dora, S., Terrett, O. M., & Sánchez-Rodríguez, C. (2022). Plant–microbe interactions in the apoplast: Communication at the plant cell wall. *The Plant Cell*, *34*(5), 1532–1550. https://doi.org/10.1093/plcell/koac040

Ellinger, D., & Voigt, C. A. (2014). Callose biosynthesis in arabidopsis with a focus on pathogen response: What we have learned within the last decade. *Annals of Botany*, *114*(6), 1349–1358. https://doi.org/10.1093/aob/mcu120

Eranthodi, A., Schneiderman, D., Harris, L. J., Witte, T. E., Sproule, A., Hermans, A., Overy, D. P., Chatterton, S., Liu, J., Li, T., Fundora, D. G.-P., Zhao, W., & Foroud, N. A. (2020). Enniatin Production Influences *Fusarium avenaceum* Virulence on Potato Tubers, but not on Durum Wheat or Peas. *Pathogens (Basel, Switzerland)*, *9*(2), 75. https://doi.org/10.3390/pathogens9020075

Fan, T., Bykova, N. V., Rampitsch, C., & Xing, T. (2016). Identification and characterization of a serine protease from wheat leaves. *European Journal of Plant Pathology*, *146*(2), 293‑304. https://doi.org/10.1007/s10658-016-0914-x

Farace, G., Fernandez, O., Jacquens, L., Coutte, F., Krier, F., Jacques, P., Clément, C., Barka, E. A., Jacquard, C., & Dorey, S. (2014). Cyclic lipopeptides fromBacillus subtilisactivate distinct patterns of defence responses in grapevine. *Molecular Plant Pathology*, *16*(2), 177–187. https://doi.org/10.1111/mpp.12170

Feigin, A. M., Schagina, L. V., Takemoto, J. Y., Teeter, J. H., & Brand, J. G. (1997). The effect of sterols on the sensitivity of membranes to the channel-forming antifungal antibiotic, syringomycin E. *Biochimica et Biophysica Acta*, *1324*(1), 102–110. https://doi.org/10.1016/s0005-2736(96)00214-3

Feiz, L., Irshad, M., Pont-Lezica, R. F., Canut, H., & Jamet, E. (2006). Evaluation of cell wall preparations for proteomics: A new procedure for purifying cell walls from Arabidopsis hypocotyls [Review of *Evaluation of cell wall preparations for proteomics: A new*

procedure for purifying cell walls from Arabidopsis hypocotyls]. *Plant Methods*, *2*(2), 10. https://doi.org/10.1186/1746-4811-2-10

Fernie, A. R., & Stitt, M. (2012). On the Discordance of Metabolomics with Proteomics and Transcriptomics: Coping with Increasing Complexity in Logic, Chemistry, and Network Interactions Scientific Correspondence. *Plant Physiology*, *158*(3), 1139–1145. https://doi.org/10.1104/pp.112.193235

Ferrari, S., Savatin, D. V., Sicilia, F., Gramegna, G., Cervone, F., & Lorenzo, G. De. (2013). Oligogalacturonides: Plant damage-associated molecular patterns and regulators of growth and development [Review of *Oligogalacturonides: Plant damage-associated molecular patterns and regulators of growth and development*]. *Frontiers in Plant Science*, *4*(49), 49. https://doi.org/10.3389/fpls.2013.00049

Frederiksen, R. F., Slettemeås, J. S., Granstad, S., Lagesen, K., Pikkemaat, M. G., Urdahl, A. M., & Simm, R. (2024). Polyether ionophore resistance in a one health perspective [Review of *Polyether ionophore resistance in a one health perspective*]. *Frontiers in Microbiology*, *15*, 1347490. https://doi.org/10.3389/fmicb.2024.1347490

Gardiner, D. M., Kazan, K., & Manners, J. M. (2009). Nutrient profiling reveals potent inducers of trichothecene biosynthesis in Fusarium graminearum. *Fungal Genetics and Biology*, *46*(8), 604–613. https://doi.org/10.1016/j.fgb.2009.04.004

Gardiner, D. M., Kazan, K., Praud, S., Torney, F. J., Rusu, A., & Manners, J. M. (2010). Early activation of wheat polyamine biosynthesis during fusarium head blight implicates putrescine as an inducer of trichothecene mycotoxin production [Review of *Early activation of wheat polyamine biosynthesis during fusarium head blight implicates*

putrescine as an inducer of trichothecene mycotoxin production]. *BMC Plant Biology*, *10*, 289. https://doi.org/10.1186/1471-2229-10-289

Garvey, G. S., McCormick, S. P., Alexander, N. J., & Rayment, I. (2009). Structural and functional characterization of TRI3 trichothecene 15-O-acetyltransferase fromFusarium sporotrichioides [Review of *Structural and functional characterization of TRI3 trichothecene 15-O-acetyltransferase fromFusarium sporotrichioides*]. *Protein Science*, *18*(4), NA–NA. https://doi.org/10.1002/pro.80

Geng, Z., Zhu, W., Su, H., Zhao, Y., Zhang, K.-Q., & Yang, J. (2014). Recent advances in genes involved in secondary metabolite synthesis, hyphal development, energy metabolism and pathogenicity in Fusarium graminearum (teleomorph Gibberella zeae). *Biotechnology Advances*, *32*(2), 390–402. https://doi.org/10.1016/j.biotechadv.2013.12.007

Getzke, F., Wang, L., Guillaume Chesneau, Nils Böhringer, Fantin Mesny, Denissen, N., Wesseler, H., Adisa, P. T., Marner, M., Schulze-Lefert, P., Schäberle, T. F., & Stéphane Hacquard. (2024). Physiochemical interaction between osmotic stress and a bacterial exometabolite promotes plant disease. *Nature Communications*, *15*(1). https://doi.org/10.1038/s41467-024-48517-5

Geudens, N., & Martins, J. C. (2018). Cyclic Lipodepsipeptides From *Pseudomonas* spp. - Biological Swiss-Army Knives [Review of *Cyclic Lipodepsipeptides From* Pseudomonas *spp. - Biological Swiss-Army Knives*]. *Frontiers in Microbiology*, *9*(1867), 1867. https://doi.org/10.3389/fmicb.2018.01867

Gibon, Y., Usadel, B., Blaesing, O. E., Kamlage, B., Hoehne, M., Trethewey, R., & Stitt, M. (2006). Integration of metabolite with transcript and enzyme activity profiling during

diurnal cycles in Arabidopsis rosettes. *Genome Biology*, *7*(8), R76. https://doi.org/10.1186/gb-2006-7-8-R76

Gilliard, G., Pršić, J., Crowet, J.-M., Chemotti, C., Ahmed, J., Lorent, J., Jolivet, M.-D., Egli, S., Egée, S., Bouyer, G., Race, G., van Buren, L., Van Den Berghe, A., Argüelles-Arias, A., Mathelié-Guinlet, M., Ibrahim, H., Genva, M., Fouillen, L., Mirande-Bret, C., … Ongena, M. (2026). Membrane remodelling mediates lipopeptide-induced immunity in Arabidopsis. *Nature Plants*, *12*(5), 1034–1050. https://doi.org/10.1038/s41477-026-02270-3

Gines, M., Baldwin, T., Rashid, A., Bregitzer, P., Maughan, P. J., Jellen, E. N., & Klos, K. E. (2018). Selection of Expression Reference Genes with Demonstrated Stability in Barley among a Diverse Set of Tissues and Cultivars. *Crop Science*, *58*(1), 332–341. https://doi.org/10.2135/cropsci2017.07.0443

Goswami, R. S., & Kistler, H. C. (2004). Heading for disaster: Fusarium graminearum on cereal crops. *Molecular Plant Pathology*, *5*(6), 515–525. https://doi.org/10.1111/j.1364-3703.2004.00252.x

Government of Canada, Canadian Food Inspection Agency, Programs, Plant Products Directorate, & Plant Breeders' Rights Office. (2017). *Canadian Food Inspection Agency - AAC Connect*. Inspection.Gc.Ca. https://active.inspection.gc.ca/english/plaveg/pbrpov/cropreport/bar/app00010044e.shtml

Gu, Y.-L., Li, J.-Z., Li, Y., Cong, S., Wang, J., Ma, Y.-N., & Wei, H.-L. (2023). Pseudomonas Cyclic Lipopeptide Medpeptin: Biosynthesis and Modulation of Plant Immunity [Review of *Pseudomonas Cyclic Lipopeptide Medpeptin: Biosynthesis and Modulation of Plant*

Immunity]. *Engineering (Beijing)*, *28*(9), 153–165. https://doi.org/10.1016/j.eng.2023.05.016

Haghpanah, M., Namdari, A., Kaleji, M. K., Nikbakht-dehkordi, A., Arzani, A., & Araniti, F. (2025). Interplay Between ROS and Hormones in Plant Defense Against Pathogens. *Plants*, *14*(9), 1297. https://doi.org/10.3390/plants14091297

Hao, G., McCormick, S., Usgaard, T., Tiley, H., & Vaughan, M. M. (2020). Characterization of Three *Fusarium graminearum* Effectors and Their Roles During Fusarium Head Blight [Review of *Characterization of Three* Fusarium graminearum *Effectors and Their Roles During Fusarium Head Blight*]. *Frontiers in Plant Science*, *11*, 579553. https://doi.org/10.3389/fpls.2020.579553

Harris, L. J., Balcerzak, M., Johnston, A., Schneiderman, D., & Ouellet, T. (2016). Host-preferential Fusarium graminearum gene expression during infection of wheat, barley, and maize. *Fungal Biology*, *120*(1), 111–123. https://doi.org/10.1016/j.funbio.2015.10.010

Hoefler, B. C., Gorzelnik, K. V., Yang, J. Y., Hendricks, N., Dorrestein, P. C., & Straight, P. D. (2012). Enzymatic resistance to the lipopeptide surfactin as identified through imaging mass spectrometry of bacterial competition. *Proceedings of the National Academy of Sciences of the United States of America*, *109*(32), 13082–13087. https://doi.org/10.1073/pnas.1205586109

Hoff, G., Anthony Argüelles Arias, Boubsi, F., Jelena Pršić, Thibault De Meyer, Ibrahim, M., Steels, S., Luzuriaga, P., Aurélien Legras, Laurent Franzil, Lequart-Pillon, M., Rayon, C., Osorio, V., Edwin De Pauw, Lara, Y., Deboever, E., Barbara De Coninck, Jacques, P., Deleu, M., … Ongena, M. (2021). Surfactin stimulated by Pectin molecular patterns and

root exudates acts as a key driver of the *bacillus* -plant mutualistic interaction. *MBio*, *12*(6). https://doi.org/10.1128/mbio.01774-21

Hoogendoorn, K., Barra, L., Waalwijk, C., Dickschat, J. S., van der Lee, T. A. J., & Medema, M. H. (2018). Evolution and Diversity of Biosynthetic Gene Clusters in Fusarium [Review of *Evolution and Diversity of Biosynthetic Gene Clusters in Fusarium*]. *Frontiers in Microbiology*, *9*. https://doi.org/10.3389/fmicb.2018.01158

Huang, P., Yu, X., Liu, H., Ding, M., Wang, Z., Xu, J.-R., & Jiang, C. (2024). Regulation of TRI5 expression and deoxynivalenol biosynthesis by a long non-coding RNA in Fusarium graminearum. *Nature Communications*, *15*(1), 1216. https://doi.org/10.1038/s41467-024-45502-w

Huang, S., Liu, Y., Liu, W.-Q., Neubauer, P., & Li, J. (2021). The nonribosomal peptide valinomycin: From Discovery to Bioactivity and biosynthesis. *Microorganisms*, *9*(4), 780. https://doi.org/10.3390/microorganisms9040780

Huang, W., Briffotaux, J., Wang, X., Liu, L., Hao, P., Cimino, M., Buchieri, M. V., Namouchi, A., Ainsa, J.-A., & Gicquel, B. (2017). Ionophore a23187 shows anti-tuberculosis activity and synergy with tebipenem. *Tuberculosis*, *107*, 111–118. https://doi.org/10.1016/j.tube.2017.09.001

Hutchison, M. L. (1995). Role of Biosurfactant and Ion Channel-Forming Activities of Syringomycin Tranransmembrane Ion Flux: A Model for the Mechanism of Action in the Plant-Pathogen Interaction. *Molecular Plant-Microbe Interactions*, *8*(4), 610. https://doi.org/10.1094/mpmi-8-0610

Hutchison, M. L., & Gross, D. C. (1997). Lipopeptide Phytotoxins Produced by Pseudomonas syringae pv. syringae: Comparison of the Biosurfactant and Ion Channel-Forming

Activities of Syringopeptin and Syringomycin. *Molecular Plant-Microbe Interactions®*, *10*(3), 347–354. https://doi.org/10.1094/mpmi.1997.10.3.347

Idone, V., Tam, C., Goss, J. W., Toomre, D., Pypaert, M., & Andrews, N. W. (2008). Repair of injured plasma membrane by rapid Ca2+ dependent endocytosis. *The Journal of Cell Biology*, *180*(5), 905–914. https://doi.org/10.1083/jcb.200708010

Ishiguro, K., & Arai, T. (1976). Action of the peptide antibiotic leucinostatin. *Antimicrobial Agents and Chemotherapy*, *9*(6), 893–898. https://doi.org/10.1128/aac.9.6.893

Jansen, C., von Wettstein, D., Schafer, W., Kogel, K.-H., Felk, A., & Maier, F. J. (2005). Infection patterns in barley and wheat spikes inoculated with wild-type and trichodiene synthase gene disrupted Fusarium graminearum. *Proceedings of the National Academy of Sciences*, *102*(46), 16892–16897. https://doi.org/10.1073/pnas.0508467102

Jelenska, J., Davern, S. M., Standaert, R. F., Mirzadeh, S., & Greenberg, J. T. (2017). Flagellin peptide flg22 gains access to long-distance trafficking in Arabidopsis via its receptor, FLS2. *Journal of Experimental Botany*, *68*(7), 1769–1783. https://doi.org/10.1093/jxb/erx060

Jenull, S., Bauer, T., Silbermayr, K., Dreer, M., Stark, T. D., & Ehling-Schulz, M. (2023). The toxicological spectrum of the *bacillus cereus* toxin cereulide points towards niche-specific specialisation. *Environmental Microbiology*, *25*(11), 2231–2249. https://doi.org/10.1111/1462-2920.16454

Jia, L.-J., Tang, H.-Y., Wang, W.-Q., Yuan, T.-L., Wei, W.-Q., Pang, B., Gong, X.-M., Wang, S.-F., Li, Y.-J., Zhang, D., Liu, W., & Tang, W.-H. (2019). A linear nonribosomal octapeptide from Fusarium graminearum facilitates cell-to-cell invasion of wheat. *Nature Communications*, *10*(1). https://doi.org/10.1038/s41467-019-08726-9

Jiang, Z., Zhou, X., Tao, M., Yuan, F., Liu, L., Wu, F., Wu, X., Xiang, Y., Niu, Y., Liu, F., Li, C., Ye, R., Byeon, B., Xue, Y., Zhao, H., Wang, H.-N., Crawford, B. M., Johnson, D. M., Hu, C., … Pei, Z.-M. (2019). Plant cell-surface GIPC sphingolipids sense salt to trigger ca2+ influx. *Nature*, *572*(7769), 341–346. https://doi.org/10.1038/s41586-019-1449-z

Jourdan, E., Henry, G., Duby, F., Dommes, J., Barthélemy, J. P., Thonart, P., & Ongena, M. (2009). Insights into the defense-related events occurring in plant cells following perception of surfactin-type lipopeptide from Bacillus subtilis. *Molecular Plant-Microbe Interactions : MPMI*, *22*(4), 456–468. https://doi.org/10.1094/MPMI-22-4-0456

Juskiw, P. E., L. Oatway, Oro, M., Nyachiro, J. M., Y. Anbessa, Xi, K., Turkington, T. K., Lohr, S., Bowness, J., & F. Capettini. (2019). Registration of 'Lowe,' a Two-Rowed Malting Barley with Enhanced Resistance to Fusarium Head Blight. *Journal of Plant Registrations*, *13*(3), 301–310. https://doi.org/10.3198/jpr2018.11.0075crc

Kevin II, D. A., Meujo, D. A., & Hamann, M. T. (2009). Polyether ionophores: Broad-spectrum and promising biologically active molecules for the control of drug-resistant bacteria and parasites. *Expert Opinion on Drug Discovery*, *4*(2), 109–146. https://doi.org/10.1517/17460440802661443

Kim, H., Son, H., & Lee, Y.-W. (2013). Effects of light on secondary metabolism and fungal development of *Fusarium graminearum*. *Journal of Applied Microbiology*, *116*(2), 380–389. https://doi.org/10.1111/jam.12381

Kolberg, L., Raudvere, U., Kuzmin, I., Adler, P., Vilo, J., & Peterson, H. (2023). G:Profiler-interoperable web service for functional enrichment analysis and gene identifier mapping (2023 update). *Nucleic Acids Research*, *51*(W1), gkad347. https://doi.org/10.1093/nar/gkad347

Kosman, O., & Kumar, R. (2015). Analysis of Effectiveness of Fungicides in Managing Downy Mildew of Grapevine. *Phytopathology*, *105*(6), 803–811. https://doi.org/10.1094/PHYTO-05-15-0118-R

Kumar, A., Karre, S., Dhokane, D., Kage, U., Hukkeri, S., & Kushalappa, A. C. (2015). Real-time quantitative PCR based method for the quantification of fungal biomass to discriminate quantitative resistance in barley and wheat genotypes to fusarium head blight [Review of *Real-time quantitative PCR based method for the quantification of fungal biomass to discriminate quantitative resistance in barley and wheat genotypes to fusarium head blight*]. *Journal of Cereal Science*, *64*, 16–22. https://doi.org/10.1016/j.jcs.2015.04.005

Le Mire, G., Siah, A., Brisset, M.-N., Gaucher, M., & Jijakli, M. H. (2018). Surfactin protects wheat against zymoseptoria tritici and activates both salicylic acid- and jasmonic acid dependent defense responses. *Agriculture*, *8*(1), 11. https://doi.org/10.3390/agriculture8010011

Li, L., Li, M., Yu, L., Zhou, Z., Liang, X., Liu, Z., Cai, G., Gao, L., Zhang, X., Wang, Y., Chen, S., & Zhou, J.-M. (2014). The FLS2-Associated Kinase BIK1 Directly Phosphorylates the NADPH Oxidase RbohD to Control Plant Immunity. *Cell Host & Microbe*, *15*(3), 329–338. https://doi.org/10.1016/j.chom.2014.02.009

Linton, K. J., Cooper, H. N., Hunter, I. S., & Leadlay, P. F. (1994). An ABC-transporter from Streptomyces longisporoflavus confers resistance to the polyether-ionophore antibiotic tetronasin. *Molecular Microbiology*, *11*(4), 777–785. https://doi.org/10.1111/j.1365-2958.1994.tb00355.x

Los, F. C. O., Kao, C.-Y., Smitham, J., McDonald, K. L., Ha, C., Peixoto, C. A., & Aroian, R. V. (2011). Rab-5- and RAB-11 dependent Vesicle-Trafficking pathways are required for Plasma membrane repair after attack by Bacterial Pore-Forming toxin. *Cell Host & Microbe*, *9*(2), 147–157. https://doi.org/10.1016/j.chom.2011.01.005

Lü, P., Liu, Y., Yu, X., Shi, C.-L., & Liu, X. (2022). The right microbe-associated molecular patterns for effective recognition by plants [Review of *The right microbe-associated molecular patterns for effective recognition by plants*]. *Frontiers in Microbiology*, *13*, 1019069. https://doi.org/10.3389/fmicb.2022.1019069

Ma, H., Liu, Y., Zhang, S., Sha, J., Sun, Y., Hu, Z., Gong, L., Dai, Y., Gao, Y., Wang, Y., & Ma, H. (2025). Wheat resistance to Fusarium head blight and breeding strategies. *Crop Health*, *3*(1). https://doi.org/10.1007/s44297-025-00048-1

Ma, T., Zhang, L., Wang, M., Li, Y., Jian, Y., Wu, L., Kistler, H. C., Ma, Z., & Yin, Y. (2021). Plant defense compound triggers mycotoxin synthesis by regulating H2B ub1 and H3K4 me2/3 deposition. *New Phytologist*, *232*(5), 2106–2123. https://doi.org/10.1111/nph.17718

Mahesh, S., Tang, K.-C., & Raj, M. (2018). Amide bond activation of Biological molecules. *Molecules*, *23*(10), 2615. https://doi.org/10.3390/molecules23102615

Manstretta, V., Morcia, C., Terzi, V., & Rossi, V. (2016). Germination ofFusarium graminearumAscospores and wheat infection are affected by Dry periods and by temperature and humidity during dry periods. *Phytopathology*, *106*(3), 262–269. https://doi.org/10.1094/phyto-05-15-0118-r

Marra, M., Camoni, L., Visconti, S., Fiorillo, A., & Evidente, A. (2021). The Surprising Story of Fusicoccin: A Wilt-Inducing Phytotoxin, a Tool in Plant Physiology and a 14-3-3-Targeted Drug. *Biomolecules*, *11*(9), 1393. https://doi.org/10.3390/biom11091393

Matthias, F., Gao, J., Morten, P., & Panstruga, R. (2021). Plant autoimmunity—fresh insights into an old phenomenon. *Plant Physiology*, *188*(3), 1419–1434. https://academic.oup.com/plphys/article/188/3/1419/6484646?login=true

McMullen, M., Bergstrom, G., De Wolf, E., Dill-Macky, R., Hershman, D., Shaner, G., & Van Sanford, D. (2012). A unified effort to fight an enemy of Wheat and barley: Fusarium head blight. *Plant Disease*, *96*(12), 1712–1728. https://doi.org/10.1094/pdis-03-12-0291-fe

Mentges, M., Glasenapp, A., Boenisch, M., Malz, S., Henrissat, B., Frandsen, R. J. N., Güldener, U., Münsterkötter, M., Bormann, J., Lebrun, M.-H., Schäfer, W., & Martinez-Rocha, A. L. (2020). Infection cushions of Fusarium graminearum are fungal arsenals for wheat infection. *Molecular Plant Pathology*, *21*(8), 1070–1087. https://doi.org/10.1111/mpp.12960

Merhej, J., Boutigny, A. L., Pinson-Gadais, L., Richard-Forget, F., & Barreau, C. (2010). Acidic pH as a determinant of TRI gene expression and trichothecene b biosynthesis in Fusarium graminearum. *Food Additives & Contaminants. Part a, Chemistry, Analysis, Control, Exposure & Risk Assessment*, *27*(5), 710–717. https://doi.org/10.1080/19440040903514531

Merhej, J., Richard-Forget, F., & Barreau, C. (2011). The pH regulatory factor pac1 regulates tri gene expression and trichothecene production in Fusarium graminearum. *Fungal*

Genetics and Biology : FG & B, *48*(3), 275–284. https://doi.org/10.1016/j.fgb.2010.11.008

Michlmayr, H., Wiesenberger, G., Rehak, K., Sopel, M., Funtak, K., Malachová, A., Fruhmann, P., Weber, J., Dufresne, M., Krska, R., Berthiller, F., & Adam, G. (2026). Culmorin inhibits detoxification of the mycotoxin deoxynivalenol by plant UDP-glucosyltransferases [Review of *Culmorin inhibits detoxification of the mycotoxin deoxynivalenol by plant UDP-glucosyltransferases*]. *Journal of Experimental Botany*, erag158. https://doi.org/10.1093/jxb/erag158

Montibus, M., Ducos, C., Bonnin-Verdal, M.-N., Bormann, J., Ponts, N., Richard-Forget, F., & Barreau, C. (2013). The bZIP Transcription Factor Fgap1 Mediates Oxidative Stress Response and Trichothecene Biosynthesis But Not Virulence in Fusarium graminearum. *PLoS ONE*, *8*(12), e83377. https://doi.org/10.1371/journal.pone.0083377

Moonjely, S., Ebert, M., Paton-Glassbrook, D., Noel, Z. A., Roze, L., Shay, R., Watkins, T., & Trail, F. (2023). Update on the state of research to manage Fusarium head blight [Review of *Update on the state of research to manage Fusarium head blight*]. *Fungal Genetics and Biology : FG & B*, *169*, 103829. https://doi.org/10.1016/j.fgb.2023.103829

Nadarajah, K. K. (2020). ROS Homeostasis in Abiotic Stress Tolerance in Plants. *International Journal of Molecular Sciences*, *21*(15), 5208. https://doi.org/10.3390/ijms21155208

Naemi, A.-O., Dey, H., Kiran, N., Sandvik, S. T., Slettemeås, J. S., Nesse, L. L., & Simm, R. (2020). NarAB Is an ABC-Type Transporter That Confers Resistance to the Polyether Ionophores Narasin, Salinomycin, and Maduramicin, but Not Monensin [Review of *NarAB Is an ABC-Type Transporter That Confers Resistance to the Polyether Ionophores*

Narasin, Salinomycin, and Maduramicin, but Not Monensin]. *Frontiers in Microbiology*, *11*(104). https://doi.org/10.3389/fmicb.2020.00104

Niu, Y., & Xiang, Y. (2018). An Overview of Biomembrane Functions in Plant Responses to High-Temperature Stress. *Frontiers in Plant Science*, *9*(915). https://doi.org/10.3389/fpls.2018.00915

Noctor, G., Mhamdi, A., Chaouch, S., Han, Y., Neukermans, J., Marquez-Garcia, B., Queval, G., & Foyer, C. H. (2012). Glutathione in plants: An integrated overview. *Plant, Cell & Environment*, *35*(2), 454–484. https://doi.org/10.1111/j.1365-3040.2011.02400.x

Oide, S., & Turgeon, B. G. (2020). Natural roles of nonribosomal peptide metabolites in fungi. *Mycoscience*, *61*(3), 101–110. https://doi.org/10.1016/j.myc.2020.03.001

O'Leary, B. M., Rico, A., McCraw, S., Fones, H. N., & Preston, G. M. (2014). The Infiltration-centrifugation Technique for Extraction of Apoplastic Fluid from Plant Leaves Using *Phaseolus vulgaris* as an Example. *Journal of Visualized Experiments*, *94*(94). https://doi.org/10.3791/52113

Ongena, M., Jourdan, E., Adam, A., Paquot, M., Brans, A., Joris, B., Arpigny, J.-L., & Thonart, P. (2007). Surfactin and fengycin lipopeptides of Bacillus subtilis as elicitors of induced systemic resistance in plants. *Environmental Microbiology*, *9*(4), 1084–1090. https://doi.org/10.1111/j.1462-2920.2006.01202.x

Pfaffl, M. W. (2001). A new mathematical model for relative quantification in real-time rt-pcr. *Nucleic Acids Research*, *29*(9), 45e–45. https://doi.org/10.1093/nar/29.9.e45

Ponts, N. (2015). Mycotoxins are a component of Fusarium graminearum stress-response system. *Frontiers in Microbiology*, *6*. https://doi.org/10.3389/fmicb.2015.01234

Ponts, N., Couedelo, L., Pinson-Gadais, L., Verdal-Bonnin, M.-N., Barreau, C., & Richard-Forget, F. (2009). Fusarium response to oxidative stress by H2O2 is trichothecene chemotype dependent. *FEMS Microbiology Letters*, *293*(2), 255–262. https://doi.org/10.1111/j.1574-6968.2009.01521.x

Ponts, N., Pinson-Gadais, L., Barreau, C., Richard-Forget, F., & Ouellet, T. (2007). Exogenous H(2)O(2) and catalase treatments interfere with Tri genes expression in liquid cultures of Fusarium graminearum. *FEBS Letters*, *581*(3), 443–447. https://doi.org/10.1016/j.febslet.2007.01.003

Power, M. (2023, November 21). *Characterization of the Gramillin Virulence Factor from Fusarium graminearum in Barley (Hordeum vulgare L.)*. Uottawa.Ca. https://ruor.uottawa.ca/items/e3047e62-095e-463c-aed7-70d81be679f1

Pršić, J., & Ongena, M. (2020). Elicitors of Plant Immunity Triggered by Beneficial Bacteria [Review of *Elicitors of Plant Immunity Triggered by Beneficial Bacteria*]. *Frontiers in Plant Science*, *11*. https://doi.org/10.3389/fpls.2020.594530

Qureshi M.K., Piotr G., Munir, S., Jindal, S., & Pavel Kerchev. (2022). Hydrogen peroxide-induced stress acclimation in plants. *Cellular and Molecular Life Sciences*, *79*(2). https://doi.org/10.1007/s00018-022-04156-x

Raaijmakers, J. M., De Bruijn, I., Ole Nybroe, & Ongena, M. (2010). Natural functions of lipopeptides from *Bacillus* and *Pseudomonas* : More than surfactants and antibiotics. *FEMS Microbiology Reviews*, *34*(6), 1037–1062. https://doi.org/10.1111/j.1574-6976.2010.00221.x

Rahman, A., Uddin, W., & Wenner, N. G. (2015). Induced systemic resistance responses in perennial ryegrass against Magnaporthe oryzae elicited by semi-purified surfactin

lipopeptides and live cells of Bacillus amyloliquefaciens. *Molecular Plant Pathology*, *16*(6), 546–558. https://doi.org/10.1111/mpp.12209

Rao, M. J., Duan, M., Zhou, C., Jiao, J., Cheng, P., Yang, L., Wei, W., Shen, Q., Ji, P., Yang, Y., Conteh, O., Yan, D., Yuan, H., Rauf, A., Ai, J., & Zheng, B. (2025). Antioxidant Defense System in Plants: Reactive Oxygen Species Production, Signaling, and Scavenging During Abiotic Stress-Induced Oxidative Damage. *Horticulturae*, *11*(5), 477. https://doi.org/10.3390/horticulturae11050477

Richter, A., Blei, F., Hu, G., Schwitalla, J. W., Lozano-Andrade, C. N., Xie, J., Jarmusch, S. A., Wibowo, M., Kjeldgaard, B., Surabhi, S., Xu, X., Jautzus, T., Phippen, C. B. W., Tyc, O., Arentshorst, M., Wang, Y., Garbeva, P., Larsen, T. O., Ram, A. F. J., … Kovács, Á. T. (2024). Enhanced surface colonisation and competition during bacterial adaptation to a fungus. *Nature Communications*, *15*(1), 4486. https://doi.org/10.1038/s41467-024-48812-1

Rokas, A., Mead, M. E., Steenwyk, J. L., Raja, H. A., & Oberlies, N. H. (2020). Biosynthetic gene clusters and the evolution of fungal chemodiversity. *Natural Product Reports*, *37*(7), 868–878. https://doi.org/10.1039/c9np00045c

Russell, J. B., & Houlihan, A. J. (2003). Ionophore resistance of ruminal bacteria and its potential impact on human health. *FEMS Microbiology Reviews*, *27*(1), 65–74. https://doi.org/10.1016/S0168-6445(03)00019-6

Schenk, S. T., & Schikora, A. (2015). Staining of callose depositions in root and leaf tissues. *Bio-Protocol*, *5*(6), e1429. https://doi.org/10.21769/BioProtoc.1429

Shwab, E. K., & Keller, N. P. (2007). Regulation of secondary metabolite production in filamentous ascomycetes. *Mycological Research*, *112*(2), 225–230. https://doi.org/10.1016/j.mycres.2007.08.021

Sieber, C. M. K., Lee, W., Wong, P., Münsterkötter, M., Mewes, H.-W., Schmeitzl, C., Varga, E., Berthiller, F., Adam, G., & Güldener, U. (2014). The Fusarium graminearum genome reveals more secondary metabolite gene clusters and hints of horizontal gene transfer. *PloS One*, *9*(10), e110311. https://doi.org/10.1371/journal.pone.0110311

Simjee, S., Heffron, A.-L., Pridmore, A., & Shryock, T. R. (2012). Reversible monensin adaptation in Enterococcus faecium, Enterococcus faecalis and Clostridium perfringens of cattle origin: Potential impact on human food safety. *The Journal of Antimicrobial Chemotherapy*, *67*(10), 2388–2395. https://doi.org/10.1093/jac/dks236

Sobrova, P., Adam, V., Vasatkova, A., Beklova, M., Zeman, L., & Kizek, R. (2010). Deoxynivalenol and its toxicity. *Interdisciplinary Toxicology*, *3*(3). https://doi.org/10.2478/v10102-010-0019-x

Svačina, P. (2005). Spring barley Radegast. *Czech Journal of Genetics and Plant Breeding*, *41*(3), 124–125. https://doi.org/10.17221/6081-CJGPB

Tanaka, K., & Heil, M. (2021). Damage-Associated Molecular Patterns (DAMPs) in Plant Innate Immunity: Applying the Danger Model and Evolutionary Perspectives [Review of *Damage-Associated Molecular Patterns (DAMPs) in Plant Innate Immunity: Applying the Danger Model and Evolutionary Perspectives*]. *Annual Review of Phytopathology*, *59*, 53–75. https://doi.org/10.1146/annurev-phyto-082718-100146

Taylor, R. W., Pfeiffer, D. R., Chapman, C. J., Craig, M. E., & Thomas, T. P. (1993). Complexation chemistry of ionophores A23187 and ionomycin. *Pure and Applied Chemistry*, *65*(3), 579–584. https://doi.org/10.1351/pac199365030579

Tempelaars, M. H., Rodrigues, S., & Abee, T. (2011). Comparative analysis of Antimicrobial activities of Valinomycin and cereulide, the bacillus cereus emetic toxin. *Applied and Environmental Microbiology*, *77*(8), 2755–2762. https://doi.org/10.1128/aem.02671-10

Waewthongrak, W., Leelasuphakul, W., & McCollum, G. (2014a). Cyclic LIPopeptides from Bacillus subtilis ABS-S14 elicit defense-related gene expression in citrus fruit. *PloS One*, *9*(10), e109386. https://doi.org/10.1371/journal.pone.0109386

Waewthongrak, W., Leelasuphakul, W., & McCollum, G. (2014b). Cyclic lipopeptides from bacillus subtilis ABS–S14 elicit Defense-Related gene expression in Citrus fruit. *PLoS One*, *9*(10), e109386. https://doi.org/10.1371/journal.pone.0109386

Wang, Y., Cao, T., Liu, D., Zhao, H., Chen, Y., Li, S., Wen, K., Ali, Q., Huang, H., Zhou, S., Wu, H., Gao, X., Tian, J., & Gu, Q. (2025). The pH signaling pathway Pal/PacC regulates fungal growth, stress responses, and mycotoxin biosynthesis in *Fusarium graminearum*. *Crop Health*, *3*(1), 17. https://doi.org/10.1007/s44297-025-00054-3

Waszczak, C., Carmody, M., & Kangasjärvi, J. (2018). Reactive oxygen species in Plant signaling. *Annual Review of Plant Biology*, *69*(1), 209–236. https://doi.org/10.1146/annurev-arplant-042817-040322

Westphal, K. R., Nielsen, K. A. H., Wollenberg, R. D., Møllehøj, M. B., Bachleitner, S., Studt, L., Lysøe, E., Giese, H., Wimmer, R., Sørensen, J. L., & Sondergaard, T. E. (2019). Fusaoctaxin A, an Example of a Two-Step Mechanism for Non-Ribosomal Peptide

Assembly and Maturation in Fungi. *Toxins*, *11*(5), 277. https://doi.org/10.3390/toxins11050277

Wipfler, R., McCormick, S. P., Proctor, R., Teresi, J., Hao, G., Ward, T., Alexander, N., & Vaughan, M. M. (2019). Synergistic Phytotoxic Effects of Culmorin and Trichothecene Mycotoxins. *Toxins*, *11*(10), 555. https://doi.org/10.3390/toxins11100555

Xiao, F., & Zhou, H. (2023). Plant salt response: Perception, signaling, and tolerance [Review of *Plant salt response: Perception, signaling, and tolerance*]. *Frontiers in Plant Science*, *13*. https://doi.org/10.3389/fpls.2022.1053699

Xue, A. G., Chen, Y., Seifert, K., Guo, W., Blackwell, B. A., Harris, L. J., & Overy, D. P. (2019). Prevalence of *Fusarium* species causing head blight of spring wheat, barley and oat in Ontario during 2001–2017. *Canadian Journal of Plant Pathology*, *41*(3), 392–402. https://doi.org/10.1080/07060661.2019.1582560

Yu, X., Feng, B., He, P., & Shan, L. (2017). From Chaos to Harmony: Responses and Signaling upon Microbial Pattern Recognition. *Annual Review of Phytopathology*, *55*(1), 109–137. https://doi.org/10.1146/annurev-phyto-080516-035649

Zeng, H.-Y., & Yao, N. (2022). Sphingolipids in plant immunity. *Phytopathology Research*, *4*(1). https://doi.org/10.1186/s42483-022-00125-1

Zhang, T., Muraih, J. K., MacCormick, B., Silverman, J., & Palmer, M. (2014). Daptomycin forms cation- and size-selective pores in model membranes. *Biochimica et Biophysica Acta*, *1838*(10), 2425–2430. https://doi.org/10.1016/j.bbamem.2014.05.014

Zheng, X.-Y., Spivey, N. W., Zeng, W., Liu, P.-P., Fu, Z. Q., Klessig, D. F., He, S. Y., & Dong, X. (2012). Coronatine promotes Pseudomonas syringae virulence in plants by activating a

signaling cascade that inhibits salicylic acid accumulation. *Cell Host & Microbe*, *11*(6), 587–596. https://doi.org/10.1016/j.chom.2012.04.014

Zhou, Y., Li, S., Qian, Q., Zeng, D., Zhang, M., Guo, L., Liu, X., Zhang, B., Deng, L., Liu, X., Luo, G., Wang, X., & Li, J. (2009). BC10, a DUF266-containing and Golgi-located type II membrane protein, is required for cell-wall biosynthesis in rice (Oryza sativa L.). *The Plant Journal : For Cell and Molecular Biology*, *57*(3), 446–462. https://doi.org/10.1111/j.1365-313X.2008.03703.x

Zhou, Z., Duan, Y., Zhang, J., Lu, F., Zhu, Y., Shim, W. B., & Zhou, M. (2021). Microtubule-assisted mechanism for toxisome assembly in Fusarium graminearum. *Molecular Plant Pathology*, *22*(2), 163–174. https://doi.org/10.1111/mpp.13015

Zhu, Z., Hao, Y., Mergoum, M., Bai, G., Humphreys, G., Cloutier, S., Xia, X., & He, Z. (2019). Breeding wheat for resistance to Fusarium head blight in the Global North: China, USA, and Canada. *The Crop Journal*, *7*(6), 730–738. https://doi.org/10.1016/j.cj.2019.06.003